

Nuclear Tomography in UPC at RHIC

- Basic pure EM process in Heavy-ion collisions
- Constrain charge radius at RHIC
 - UPC
 - Centrality
 - beam energy dependence
- Final-state EM field
- Spin Interference Enabled Nuclear Tomography (nuclear mass radius)

J.D. Brandenburg, seminar, week 5

INT workshop 02/07/2023

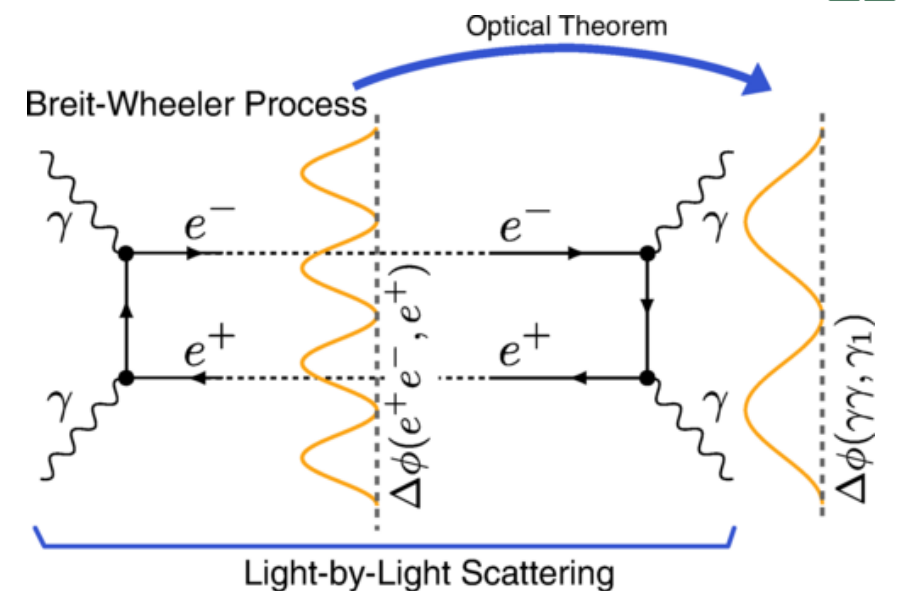
Zhangbu Xu



- [arXiv:1806.02295](#) PRL
- [arXiv:1804.01813](#) PLB
- [arXiv:1705.01460](#) PRC
- [arXiv:1812.02820](#) PLB
- [arXiv:1910.12400](#) PRL
- [arXiv:2103.16623](#) EPJA
- [arXiv:2207.05595](#) PRC
- [arXiv:2204.01626](#) SA
- [arXiv:2208.14943](#) ROPP
- [STAR BUR 2021-2025](#)

Measurement of e^+e^- Momentum and Angular Distributions from Linearly Polarized Photon Collisions

J. Adam et al. (STAR Collaboration)
Phys. Rev. Lett. **127**, 052302 – Published 27 July 2021



Two-photon QED in Particle Data Book

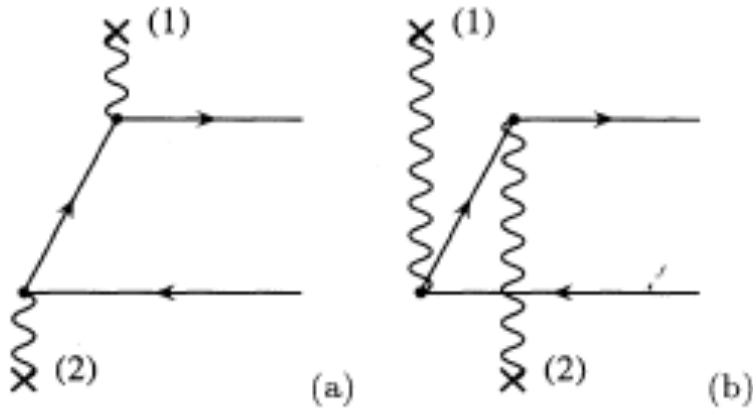
51.7 Two-photon processes

In the Weizsäcker-Williams picture, a high-energy electron beam is accompanied by a spectrum of virtual photons of energies ω and invariant-mass squared $q^2 = -Q^2$, for which the photon number density is

$$dn = \frac{\alpha}{\pi} \left[1 - \frac{\omega}{E} + \frac{\omega^2}{E^2} - \frac{m_e^2 \omega^2}{Q^2 E^2} \right] \frac{d\omega}{\omega} \frac{dQ^2}{Q^2}, \quad (51.43)$$

where E is the energy of the electron beam. The cross section for $e^+e^- \rightarrow e^+e^-X$ is then [9]

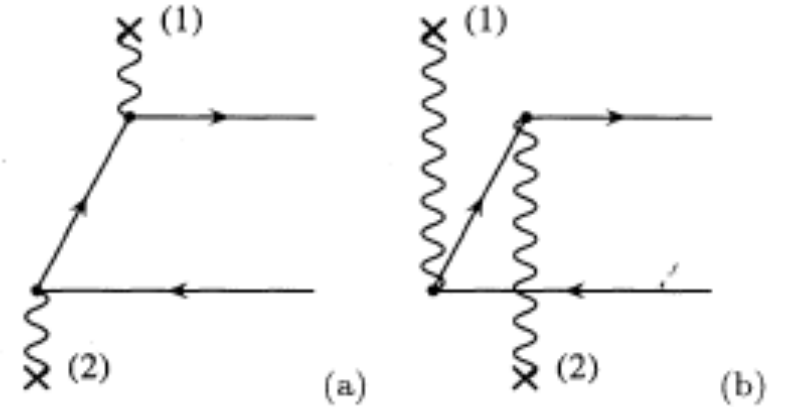
$$d\sigma_{e^+e^- \rightarrow e^+e^-X}(s) = dn_1 dn_2 d\sigma_{\gamma\gamma \rightarrow X}(W^2), \quad (51.44)$$



Natural extension to Heavy Ions

$$\rho_A(r) = \frac{\rho^0}{1 + \exp[(r - R_{WS})/d]}$$

$$dn_i = \frac{Z_i^2 \alpha}{\pi^2} \frac{q_{i\perp}^2 \left[F \left(q_{i\perp}^2 + \frac{w_i^2}{\gamma^2} \right) \right]^2}{\left(q_{i\perp}^2 + \frac{w_i^2}{\gamma^2} \right)^2} \frac{d^3 q_i}{w_i} \quad (1)$$

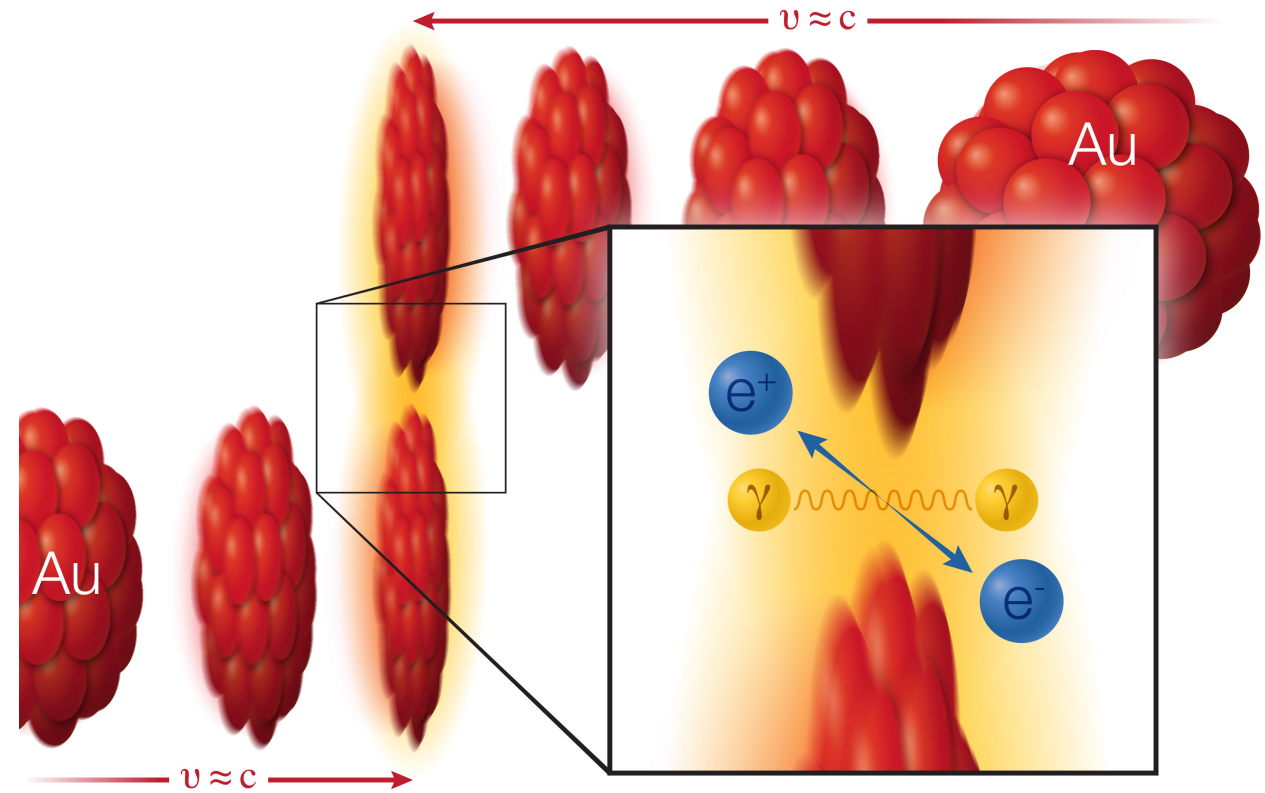
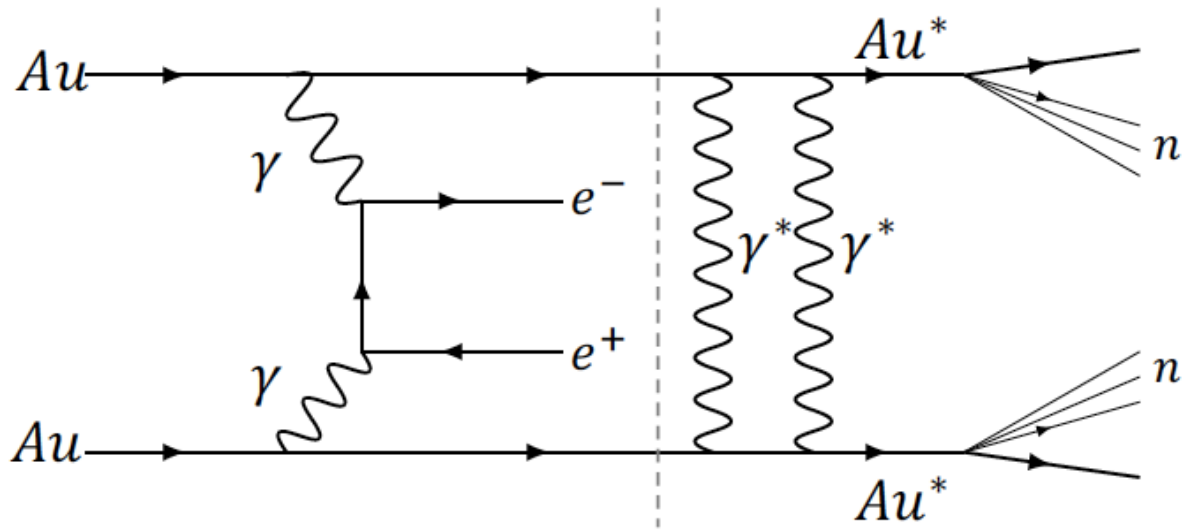


$$\sigma = 16 \frac{Z^4 e^4}{(4\pi)^2} \int \frac{dw_1}{w_1} \frac{dw_2}{w_2} \frac{d^2 k_{1\perp}}{(2\pi)^2} \frac{d^2 k_{2\perp}}{(2\pi)^2} \left| \frac{F(-k_1^2)}{k_1^2} \right|^2 \times \left| \frac{F(-k_2^2)}{k_2^2} \right|^2 k_{1\perp}^2 k_{2\perp}^2 \sigma(w_1, w_2) \quad (6)$$

arXiv:1005.3531, unpublished

S. Klein, et al. Comput.Phys.Commun. 212 (2017) 258-268

First, some basics of the Breit-Wheeler process



Two gold (Au) ions (red) move in opposite direction at 99.995% of the speed of light (v , for velocity, = approximately c , the speed of light). As the ions pass one another without colliding, two photons (γ) from the electromagnetic cloud surrounding the ions can interact with each other to create a matter-antimatter pair: an electron (e^-) and positron (e^+).

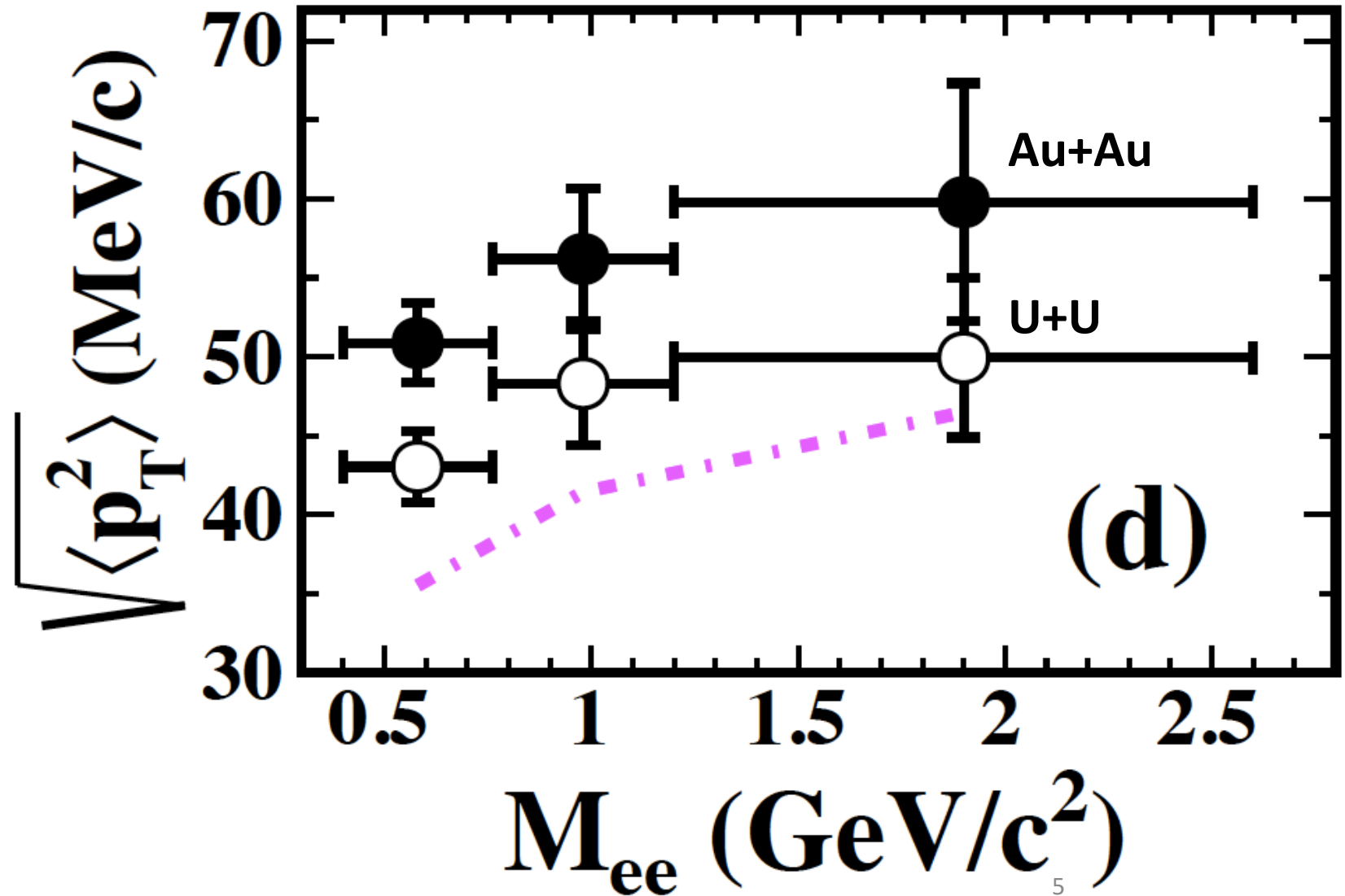
p_T broadening

Two Issues:

p_T spread (σ_t) > Model
additional broadening of
40MeV

Au+Au > U+U

Why “broadening”:
Gaussian in p_T



p_T broadening

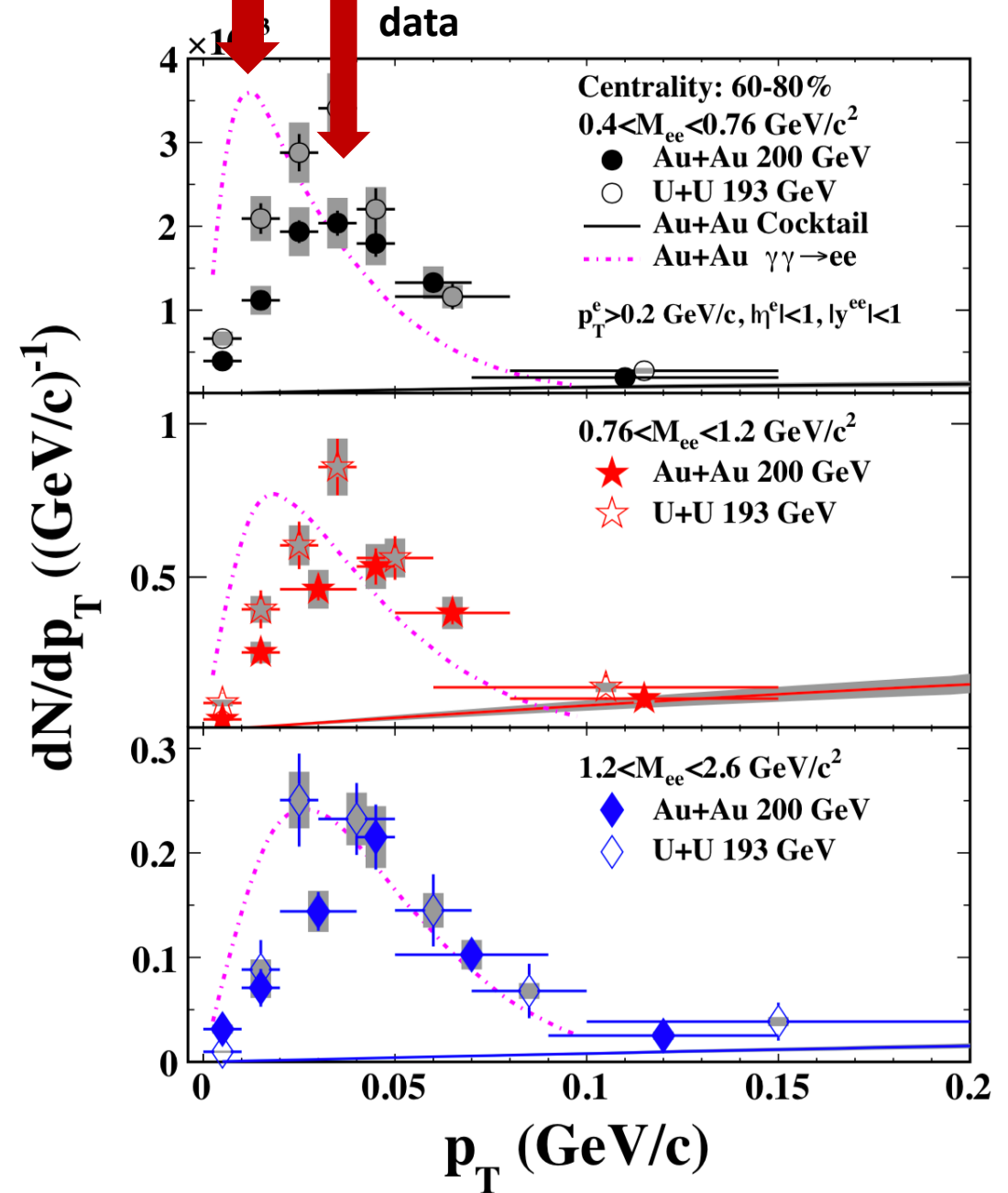
Two Issues:

p_T spread (σ_t) > Model
additional broadening of
40MeV

Au+Au > U+U

Why “broadening”:
Gaussian in p_T

STARlight Model




What did STAR say in the publication?

PHYSICAL REVIEW LETTERS **121**, 132301 (2018)

Low- p_T e^+e^- Pair Production in Au + Au Collisions at $\sqrt{s_{NN}} = 200$ GeV and U + U Collisions at $\sqrt{s_{NN}} = 193$ GeV at STAR

PHYSICAL REVIEW LETTERS **121**, 132301 (2018)

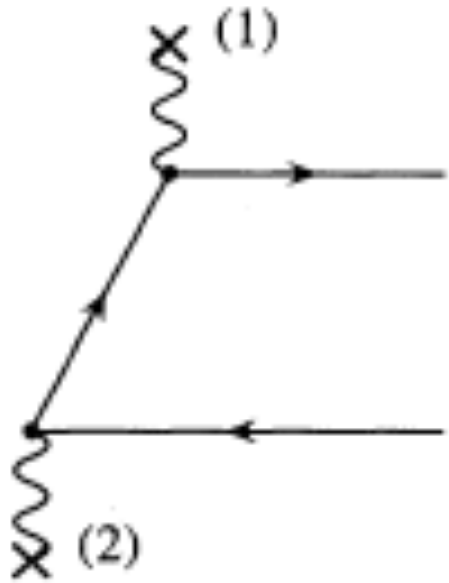
 (Received 6 June 2018; revised manuscript received 30 August 2018; published 25 September 2018)

We report first measurements of e^+e^- pair production in the mass region $0.4 < M_{ee} < 2.6$ GeV/ c^2 at low transverse momentum ($p_T < 0.15$ GeV/ c) in noncentral Au + Au collisions at $\sqrt{s_{NN}} = 200$ GeV and U + U collisions at $\sqrt{s_{NN}} = 193$ GeV. Significant enhancement factors, expressed as ratios of data over known hadronic contributions, are observed in the 40%–80% centrality of these collisions. The excess yields peak distinctly at low p_T with a width ($\sqrt{\langle p_T^2 \rangle}$) between 40 and 60 MeV/ c . The absolute cross section of the excess depends weakly on centrality, while those from a theoretical model calculation incorporating an in-medium broadened ρ spectral function and radiation from a quark gluon plasma or hadronic cocktail contributions increase dramatically with an increasing number of participant nucleons. Model calculations of photon-photon interactions generated by the initial projectile and target nuclei describe the observed excess yields but fail to reproduce the p_T^2 distributions.

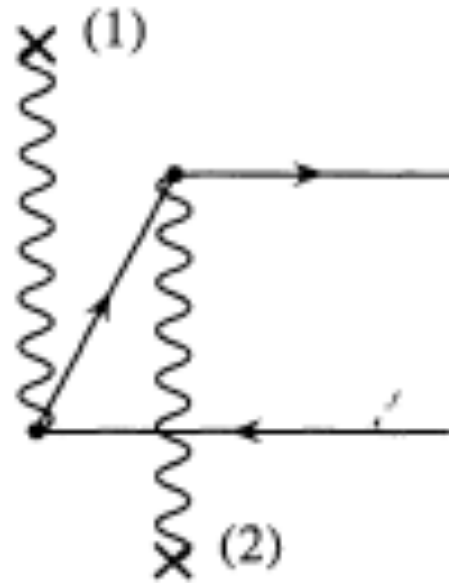
DOI: [10.1103/PhysRevLett.121.132301](https://doi.org/10.1103/PhysRevLett.121.132301)

Fig. 4(d). For example, to illustrate the sensitivity the $\sqrt{\langle p_T^2 \rangle}$ measurement may have to a postulated magnetic field trapped in a conducting QGP [21], we assume each and every pair member generated by model [33] traverses 1 fm through a constant magnetic field of 10^{14} T perpendicular to the beam line ($eBL \approx 30$ MeV/ c , where B is 10^{14} T, L is 1 fm) [37, 38]. The corresponding p_T^2 distributions of e^+e^- pairs can qualitatively describe our data except at low p_T^2 , as shown in Figs. 4(a)-(c). The $\sqrt{\langle p_T^2 \rangle}$ of e^+e^- pairs will gain an additional ~ 30 MeV/ c , as illustrated in Fig. 4(d). This level of broadening is measurable and may indicate the possible existence of high magnetic fields [21, 37, 38].

Lowest-order QED calculation



(a)



(b)

$$\sigma = \int d^2b \frac{d^6 P(\vec{b})}{d^3p_+ d^3p_-} = \int d^2q \frac{d^6 P(\vec{q})}{d^3p_+ d^3p_-} \int d^2b e^{i\vec{q}\cdot\vec{b}}$$

$$\begin{aligned} \frac{d^6 P(\vec{q})}{d^3p_+ d^3p_-} &= (Z\alpha)^4 \frac{4}{\beta^2} \frac{1}{(2\pi)^6 2\epsilon_+ 2\epsilon_-} \int d^2q_1 \\ &F(N_0)F(N_1)F(N_3)F(N_4)[N_0N_1N_3N_4]^{-1} \\ &\times \text{Tr}\{(\not{p}_- + m)[N_{2D}^{-1}\not{\psi}_1(\not{p}_- - \not{q}_1 + m)\not{\psi}_2 + \\ &N_{2X}^{-1}\not{\psi}_2(\not{q}_1 - \not{p}_+ + m)\not{\psi}_1](\not{p}_+ - m)[N_{5D}^{-1}\not{\psi}_2 \\ &(\not{p}_- - \not{q}_1 - \not{q} + m)\not{\psi}_1 + N_{5X}^{-1}\not{\psi}_1(\not{q}_1 + \not{q} - \not{p}_+ \\ &+ m)\not{\psi}_2]\}, \end{aligned}$$

with

$$\begin{aligned} N_0 &= -q_1^2, N_1 = -[q_1 - (p_+ + p_-)]^2, \\ N_3 &= -(q_1 + q)^2, N_4 = -[q + (q_1 - p_+ - p_-)]^2, \\ N_{2D} &= -(q_1 - p_-)^2 + m^2, \\ N_{2X} &= -(q_1 - p_+)^2 + m^2, \\ N_{5D} &= -(q_1 + q - p_-)^2 + m^2, \\ N_{5X} &= -(q_1 + q - p_+)^2 + m^2, \end{aligned}$$

Initial Transverse Momentum Broadening

$$\begin{aligned} \sigma = & 16 \frac{Z^4 e^4}{(4\pi)^2} \int d^2b \int \frac{dw_1}{w_1} \frac{dw_2}{w_2} \frac{d^2k_{1\perp}}{(2\pi)^2} \frac{d^2k_{2\perp}}{(2\pi)^2} \frac{d^2q_{\perp}}{(2\pi)^2} \\ & \times \frac{F(-k_1^2)}{k_1^2} \frac{F(-k_2^2)}{k_2^2} \frac{F^*(-k_1'^2)}{k_1'^2} \frac{F^*(-k_2'^2)}{k_2'^2} e^{-i\vec{b}\cdot\vec{q}_{\perp}} \\ & \times [(\vec{k}_{1\perp} \cdot \vec{k}_{2\perp})(\vec{k}'_{1\perp} \cdot \vec{k}'_{2\perp})\sigma_s(w_1, w_2) \\ & + (\vec{k}_{1\perp} \times \vec{k}_{2\perp})(\vec{k}'_{1\perp} \times \vec{k}'_{2\perp})\sigma_{ps}(w_1, w_2)] \end{aligned} \quad (2)$$

Zha, et al., arXiv: 1812.02820

M. Vidovic, et al., Phys.Rev. C47 (1993) 2308

$$\rho_A(r) = \frac{\rho^0}{1 + \exp[(r - R_{WS})/d]}$$

$$dn_i = \frac{Z_i^2 \alpha}{\pi^2} \frac{q_{i\perp}^2 \left[F\left(q_{i\perp}^2 + \frac{w_i^2}{\gamma^2}\right) \right]^2}{\left(q_{i\perp}^2 + \frac{w_i^2}{\gamma^2}\right)^2} \frac{d^3q_i}{w_i} \quad (1)$$

arXiv:1005.3531, unpublished

$$\begin{aligned} \sigma = & 16 \frac{Z^4 e^4}{(4\pi)^2} \int \frac{dw_1}{w_1} \frac{dw_2}{w_2} \frac{d^2k_{1\perp}}{(2\pi)^2} \frac{d^2k_{2\perp}}{(2\pi)^2} \left| \frac{F(-k_1^2)}{k_1^2} \right|^2 \\ & \times \left| \frac{F(-k_2^2)}{k_2^2} \right|^2 k_{1\perp}^2 k_{2\perp}^2 \sigma(w_1, w_2) \end{aligned} \quad (6)$$

S. Klein, et al. Comput.Phys.Commun. 212 (2017) 258-268

Is photon pt really driven by uncertainty principle and independent of position-momentum correlation?

we can afford many mistakes in the search.
The main thing is to make them as fast as possible.

– John Archibald Wheeler

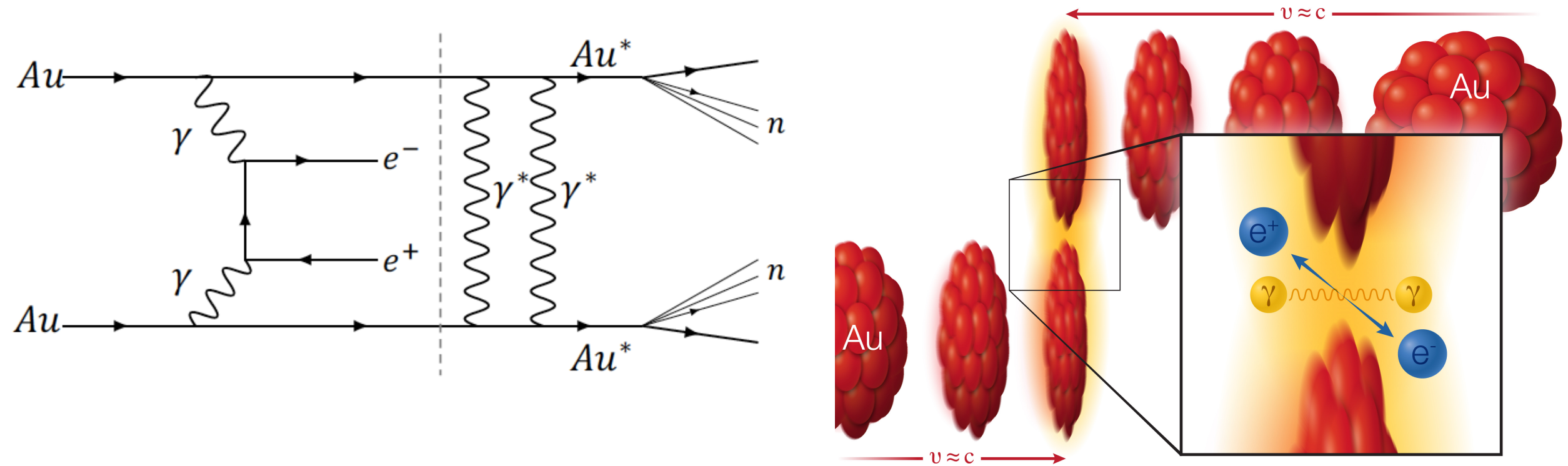
[doi:10.1063/1.3120895](https://doi.org/10.1063/1.3120895)

$\omega/\gamma \lesssim kt \ll \omega$

Higher-order/virtuality cancels to $1/\gamma^2 \sim 10^{-4}$

NLO QED coupling constant $\alpha=1/137$

Ultra-Peripheral Collisions



Two gold (Au) ions (red) move in opposite direction at 99.995% of the speed of light (v , for velocity, = approximately c , the speed of light). As the ions pass one another without colliding, two photons (γ) from the electromagnetic cloud surrounding the ions can interact with each other to create a matter-antimatter pair: an electron (e^-) and positron (e^+).

Baseline QED process in UPC

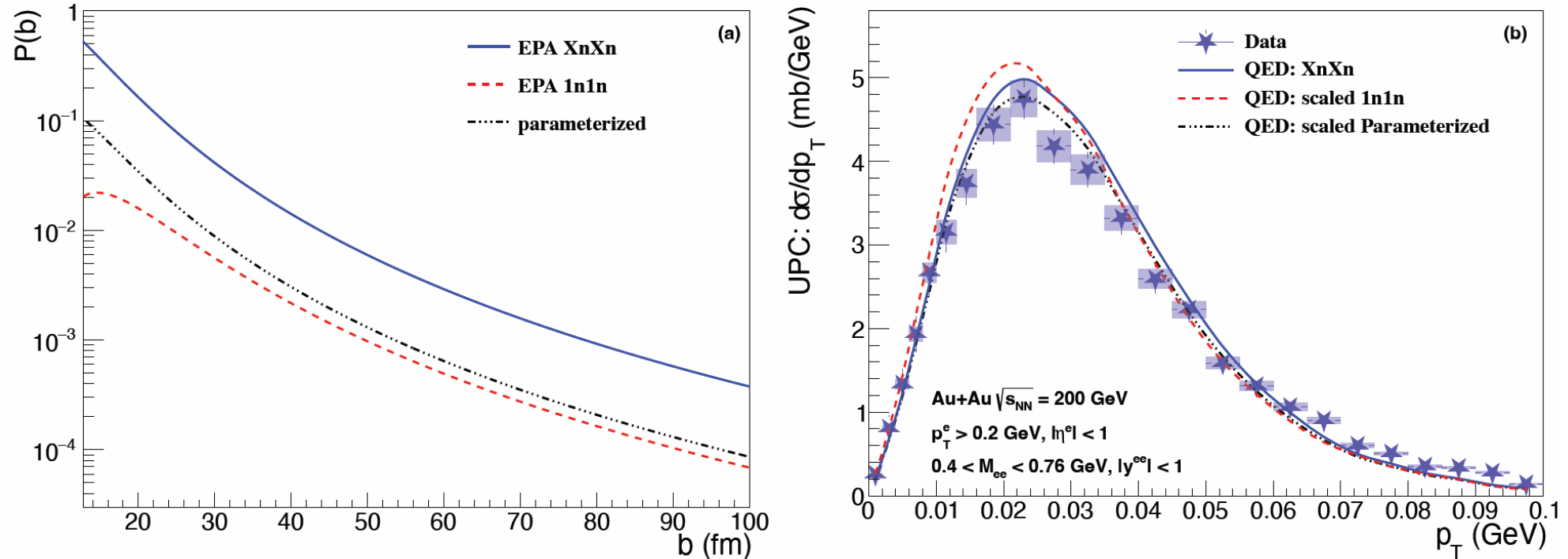
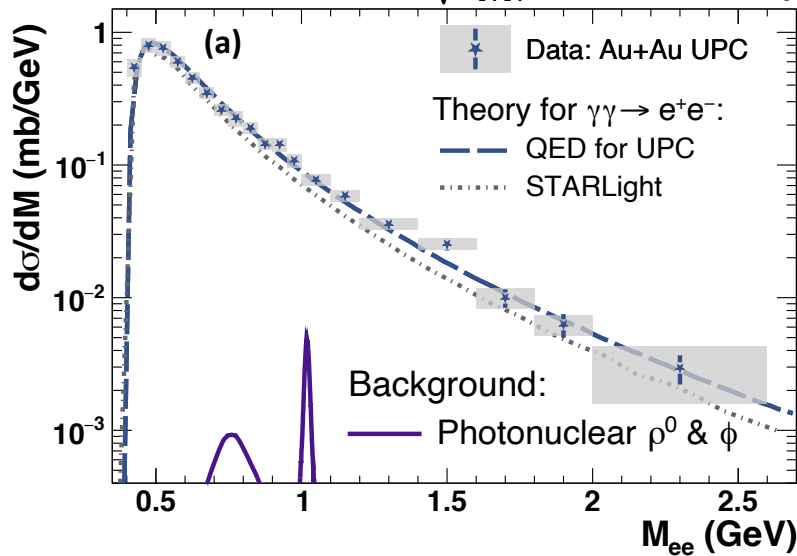


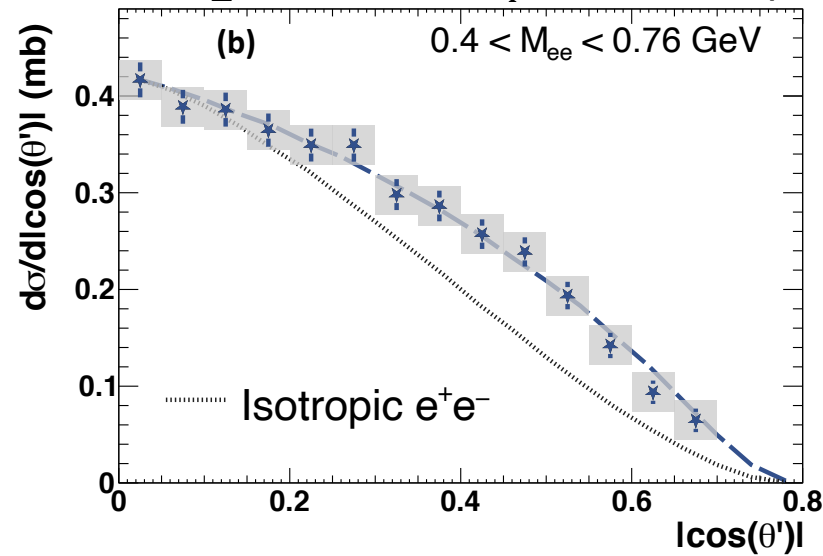
FIG. 1. (color online) (a) The nucleus break-up probability of Au as a function of impact parameter for different number of neutron emission and parametrizations. (b) Differential cross sections as functions of dielectron transverse momenta for different probability of neutron emission compared to STAR measurement [23] with neutron selection condition XnXn in Au+Au UPCs at 200 GeV.

Well understood kinematics

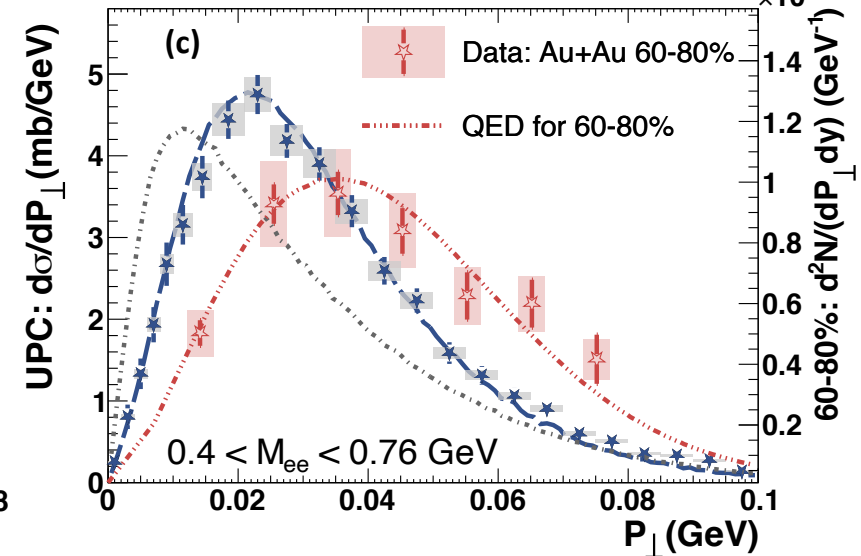
STAR: Au+Au at $\sqrt{s_{NN}} = 200$ GeV, $|y^{ee}| < 1$, $P_{\perp} < 0.1$ GeV, $P_T^e > 0.2$ GeV, $|\eta^e| < 1$, Overall scale uncertainty $\pm 13\%$



$\rho, \phi, \omega < \pm 0.2\%$



$< \pm 2\%$



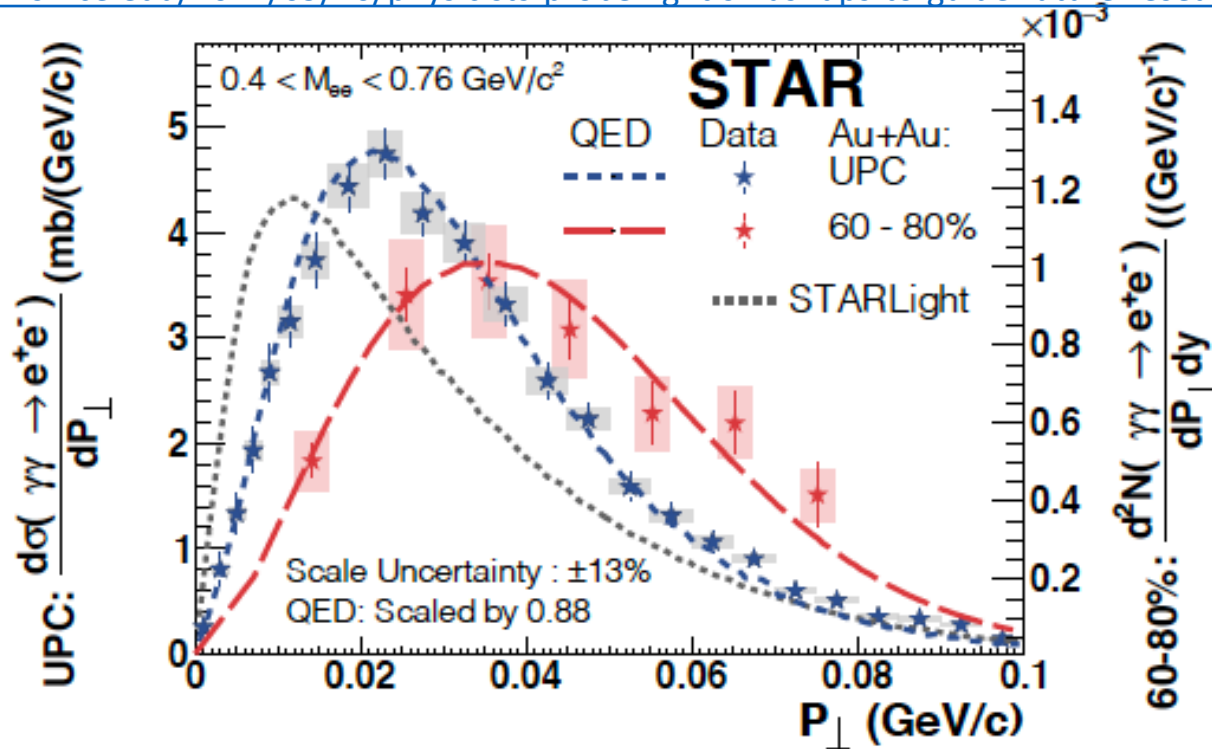
$< \pm 2\%$

photon p_T is simply due to finite electric field projection in the longitudinal direction, It is classic EM field and not due to uncertainty principle of $R \cdot p_T \sim \hbar$

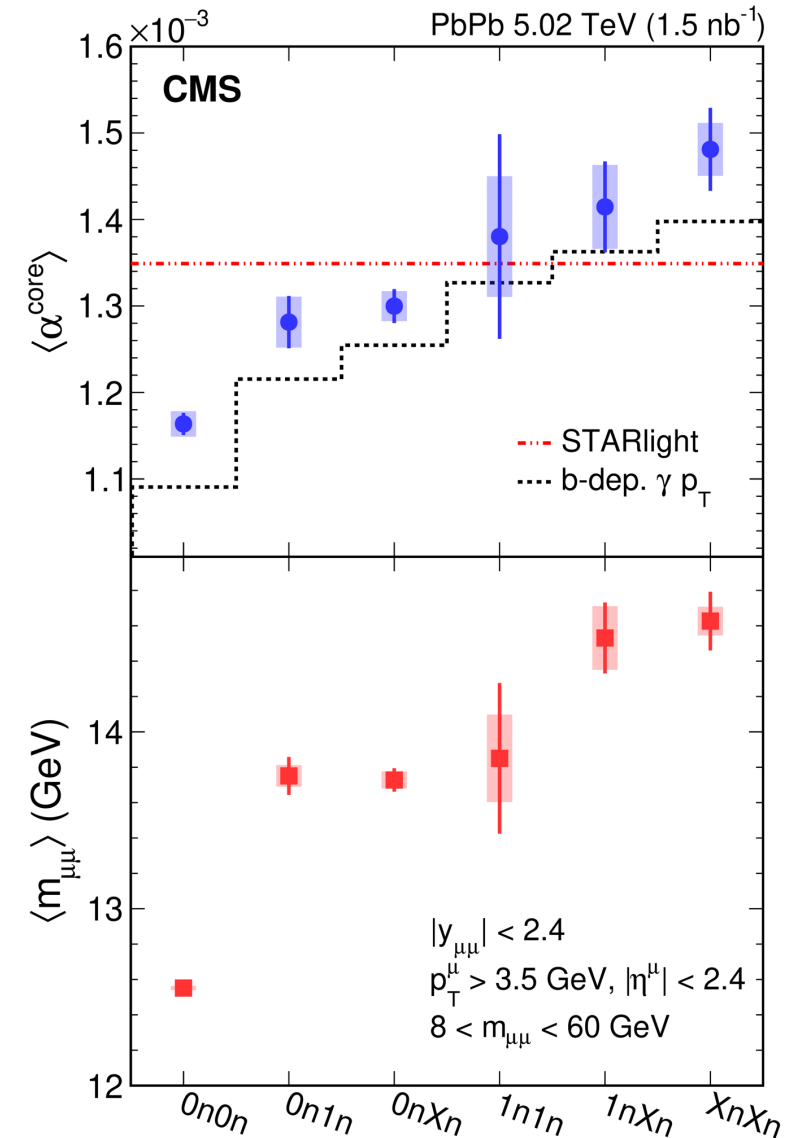
Photon TMD in UPC

CMS Abstract: “This observation demonstrates the transverse momentum and energy of photons emitted from relativistic ions have impact parameter dependence. These results constrain precision modeling of initial photon-induced interactions in ultra-peripheral collisions. They also provide a controllable baseline to search for possible final-state effects on lepton pairs resulting from the production of quark-gluon plasma in hadronic heavy ion collisions.”

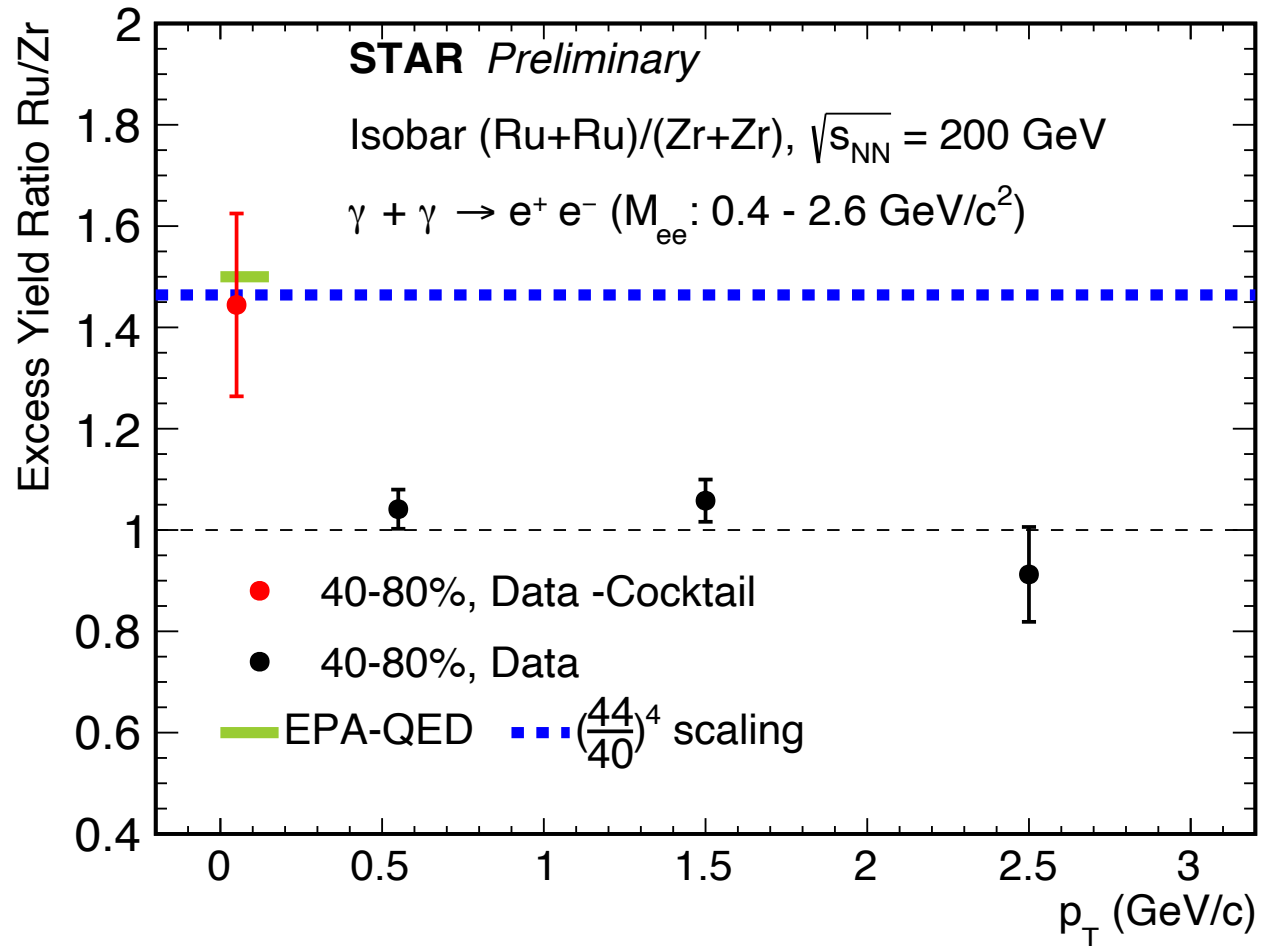
<https://news.rice.edu/2021/09/20/physicists-probe-light-smashups-to-guide-future-research-2/>



- 50. STAR Collaboration, J., Adam *et al.* Probing Extreme Electromagnetic Fields with the Breit-Wheeler Process. (2019). <https://arxiv.org/abs/1910.12400>.
- 51. ATLAS Collaboration. Measurement of non-exclusive dimuon pairs produced via $\gamma\gamma$ scattering in Pb+Pb collisions at $\sqrt{s_{NN}} = 5.02 \text{ TeV}$ with the ATLAS detector. ATLAS-CONF-2019-051. (2019). <https://inspirehep.net/literature/1762955>.
- 52. CMS Collaboration,. Observation of forward neutron multiplicity dependence of dimuon acoplanarity in ultra-peripheral PbPb collisions at $\sqrt{s_{NN}} = 5.02 \text{ TeV}$ CMS-PAS-HIN-19-014. (2020). <https://inspirehep.net/literature/1798862>.



Experimental Constraints on Initial EM Fields



- How well are the initial EM fields really known?
- Do event by-event fluctuations wash out differences?

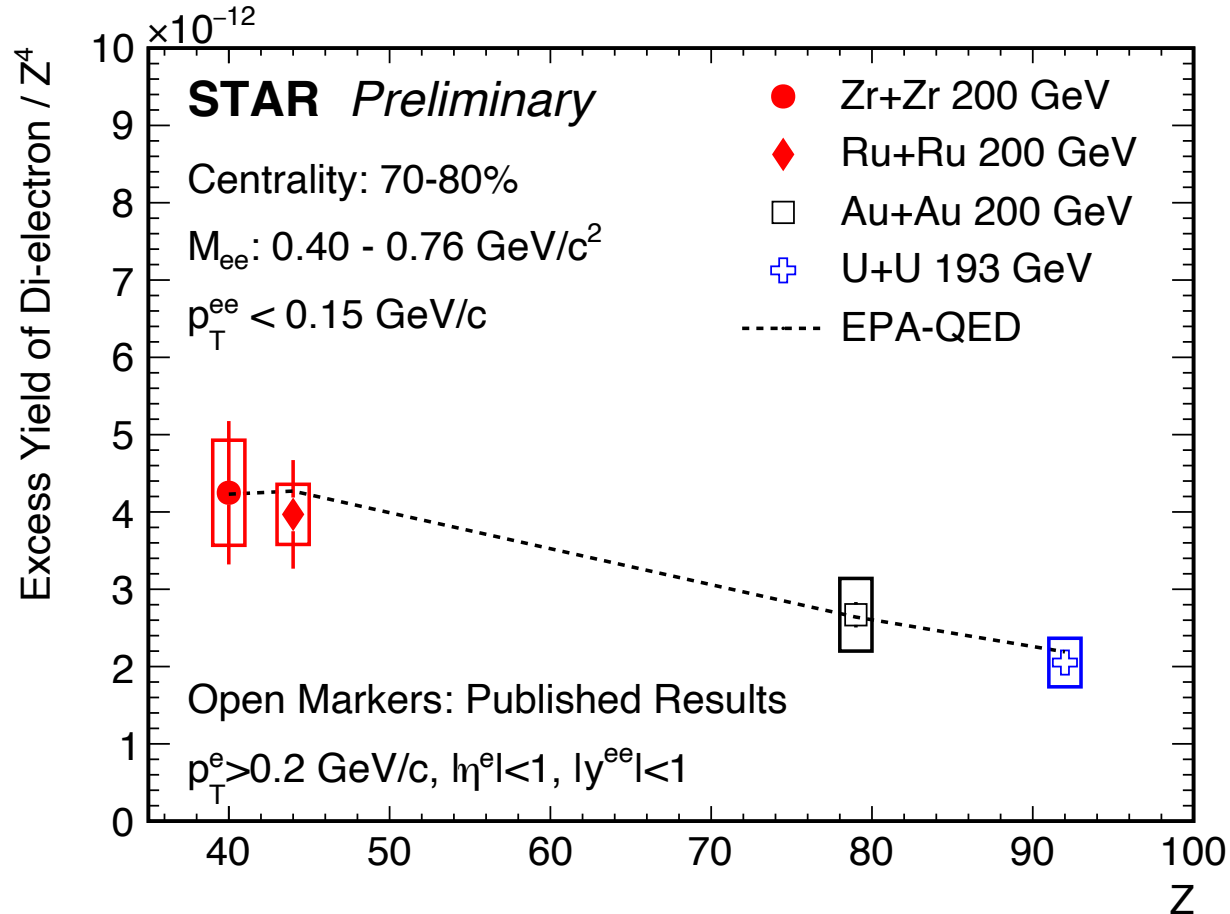
Ratio is consistent with $(\frac{44}{40})^4$ at very low p_T

Initial EM field is different in Ru + Ru and Zr + Zr ($\sim 3\sigma$)

Au+Au, U+U large level arm Z^4

Kaifeng Shen (USTC)

Experimental Constraints on Initial EM Fields



- How well are the initial EM fields really known?
- Do event by-event fluctuations wash out differences?

Ratio is consistent with $\left(\frac{44}{40}\right)^4$ at very low p_T

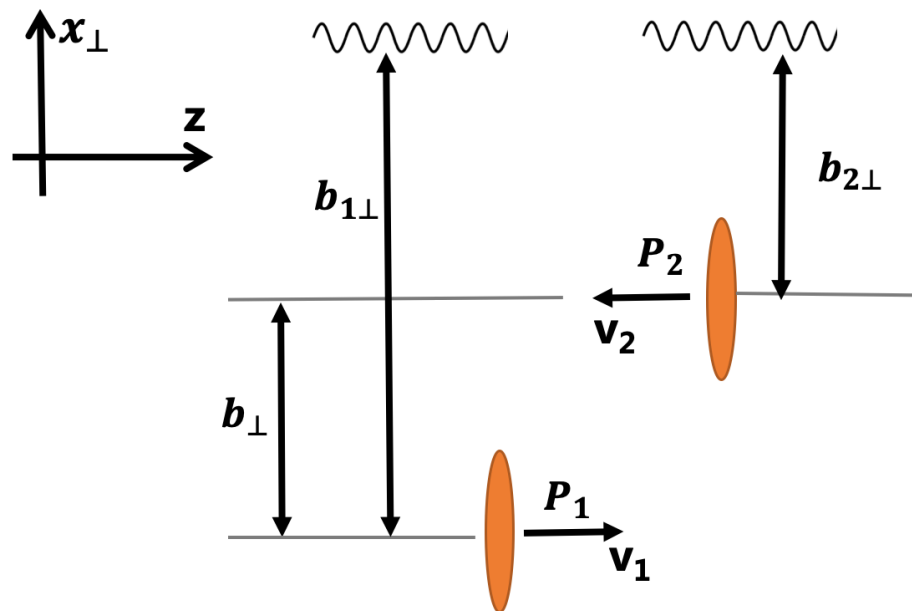
Initial EM field is different in Ru + Ru and Zr + Zr ($\sim 3\sigma$)

Au+Au, U+U large level arm Z^4

Kaifeng Shen (USTC)

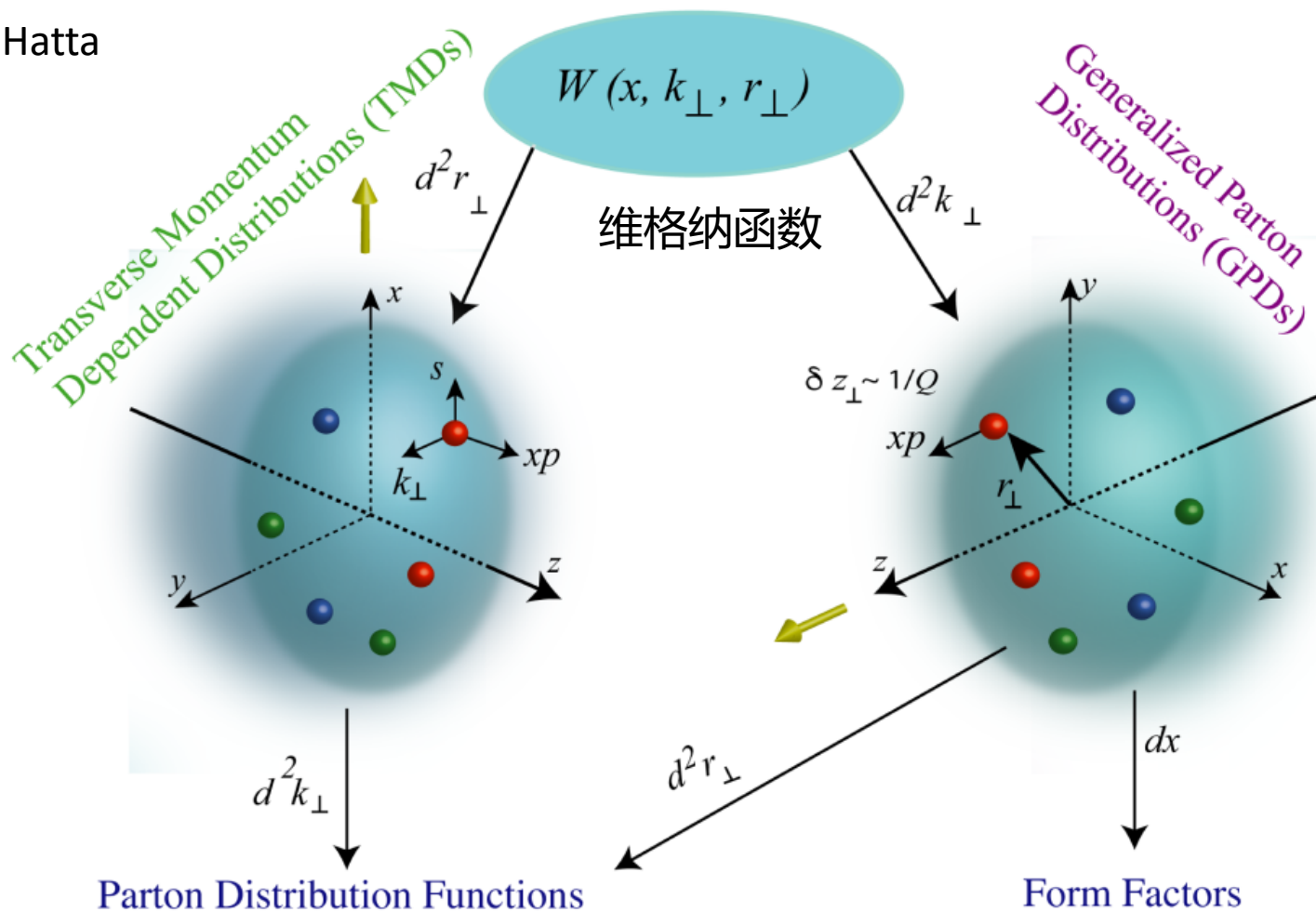
Quite a few techniques used in QCD can be used in strong-field QED as well

Understanding the QED is also important for quantitative extraction of the photoproduction



Y. Hatta

Wigner Distributions



Wang/Pu/Wang, PRD, <https://arxiv.org/pdf/2106.05462.pdf>

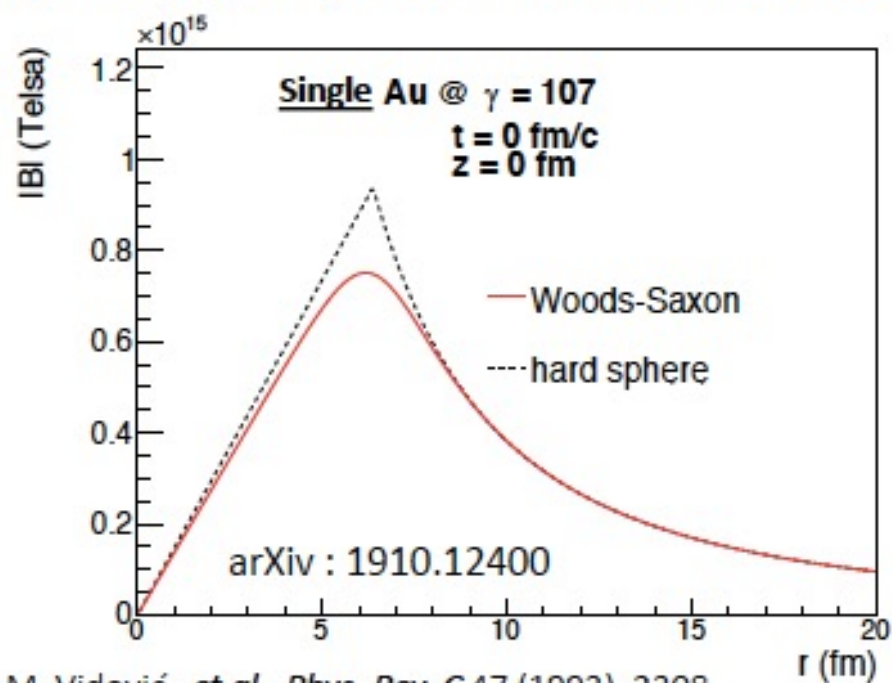
Application : Mapping the Magnetic Field

Total and differential cross-sections (e.g. $d\sigma/dP_{\perp}$) for $\gamma\gamma \rightarrow e^+e^-$ are related to field strength and configuration

photon density is related to energy flux of the electromagnetic fields [1]

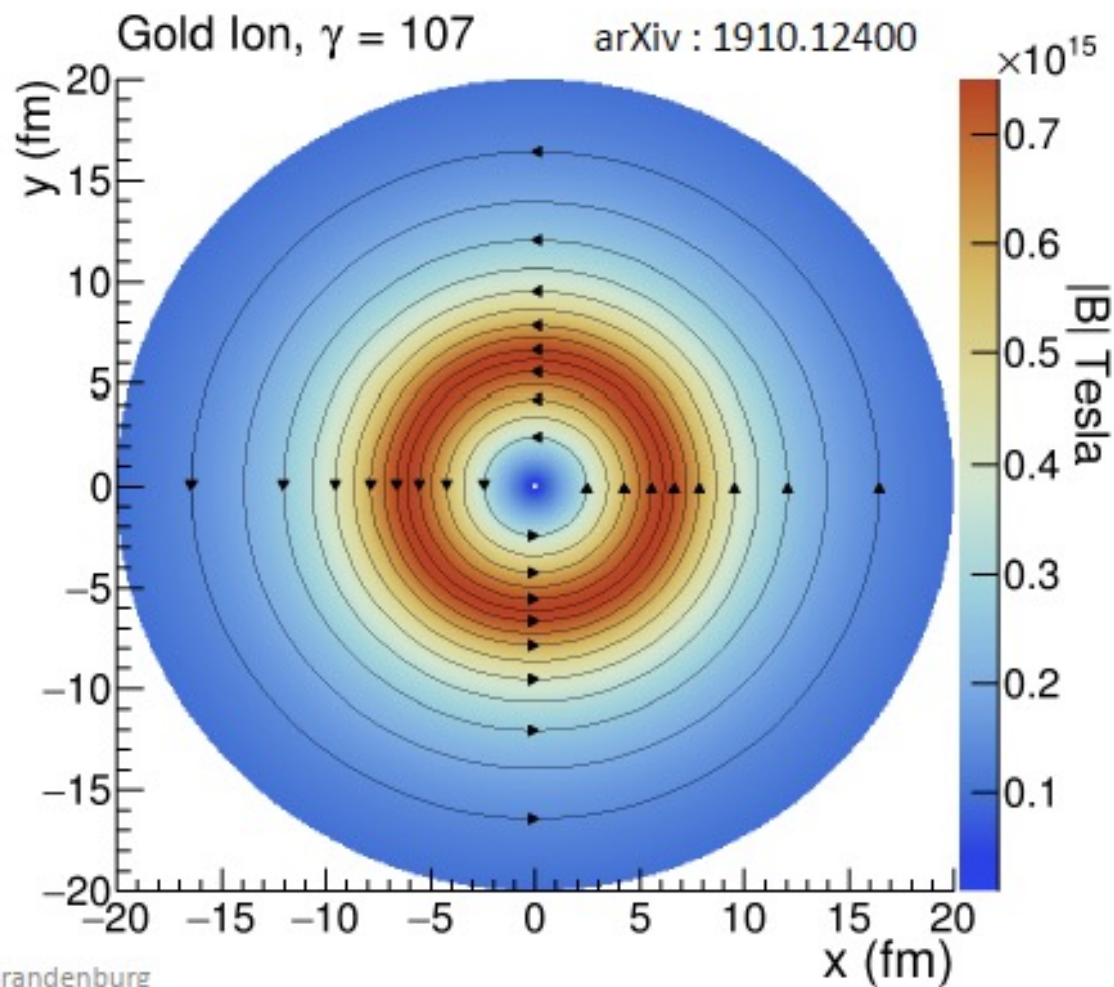
$$n \propto \vec{S} = \frac{1}{\mu_0} \vec{E} \times \vec{B}$$

→ Report \vec{B} (single ion) that matches measured cross-section



[1] M. Vidović, et al., *Phys. Rev. C* 47 (1993), 2308

11/05/19



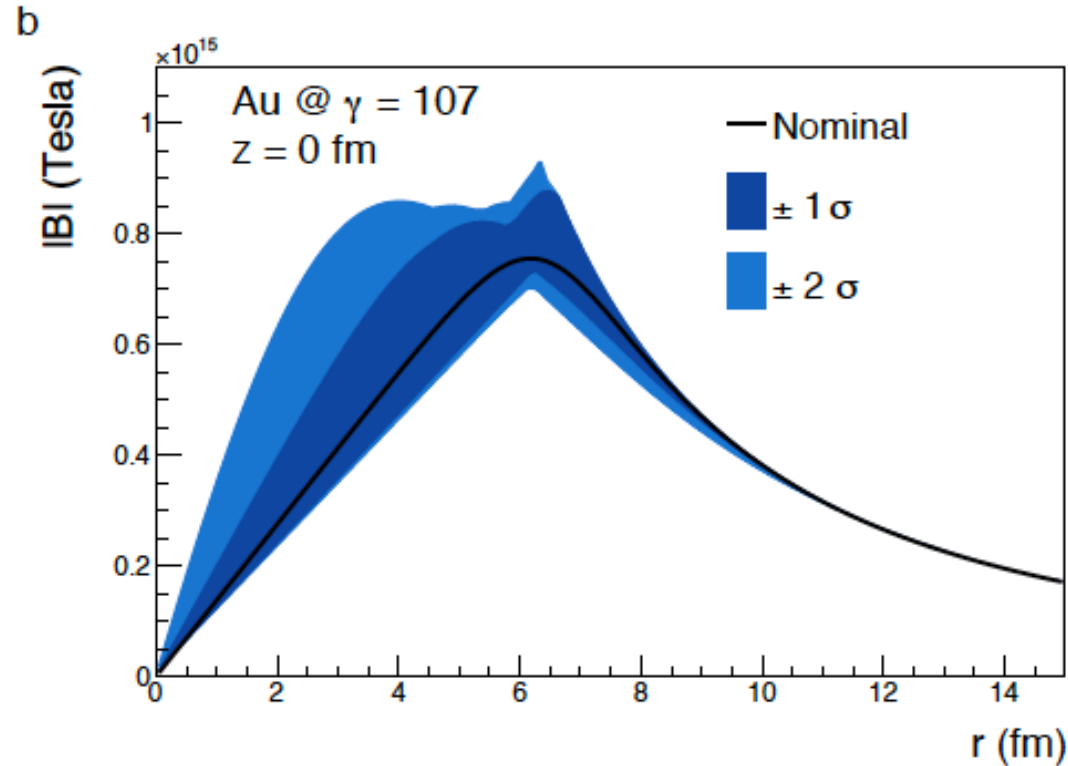
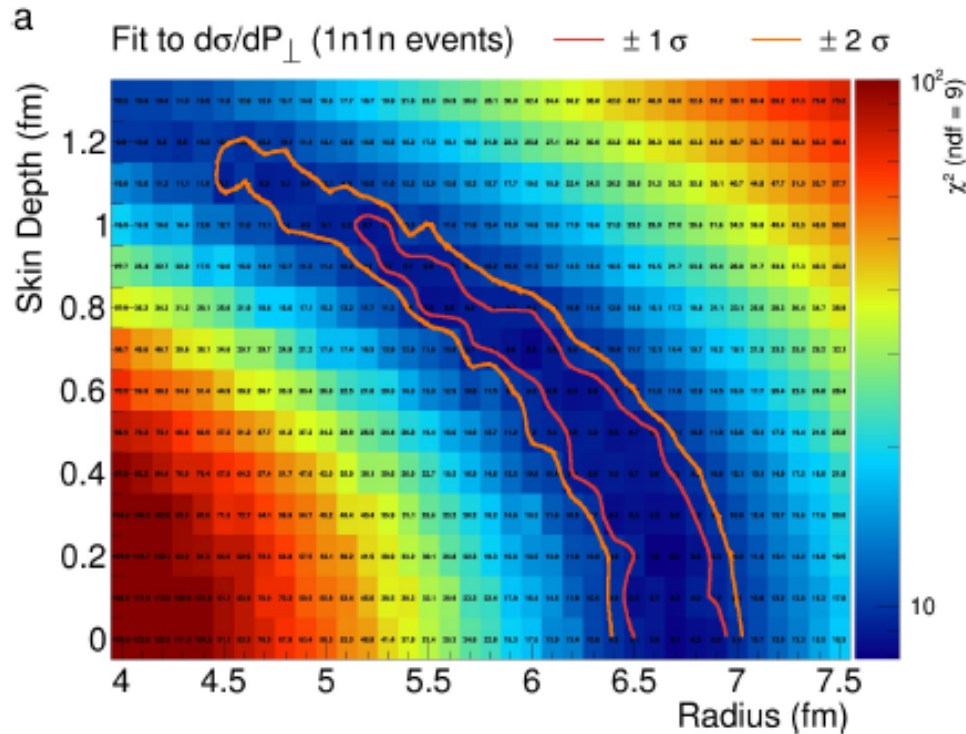
Daniel Brandenburg

14

Mapping of EM Field Distribution

STAR, arXiv : 1910.12400
JDB, W Zha, Z Xu, arXiv:2103.16623

Precision transverse momentum + polarization = constrain field spatial extent



- Much stronger field possible at small distances
 - More measurements needed to constrain event-by-event fluctuations of EM fields
- **Novel input for magnetic-field driven phenomena**

Constraint on charge distribution with precision

Using LO QED to calculate Breit-Wheeler process to match data with least-chi2

UPC consistent with nominal nuclear geometry

Peripheral collisions systematically larger

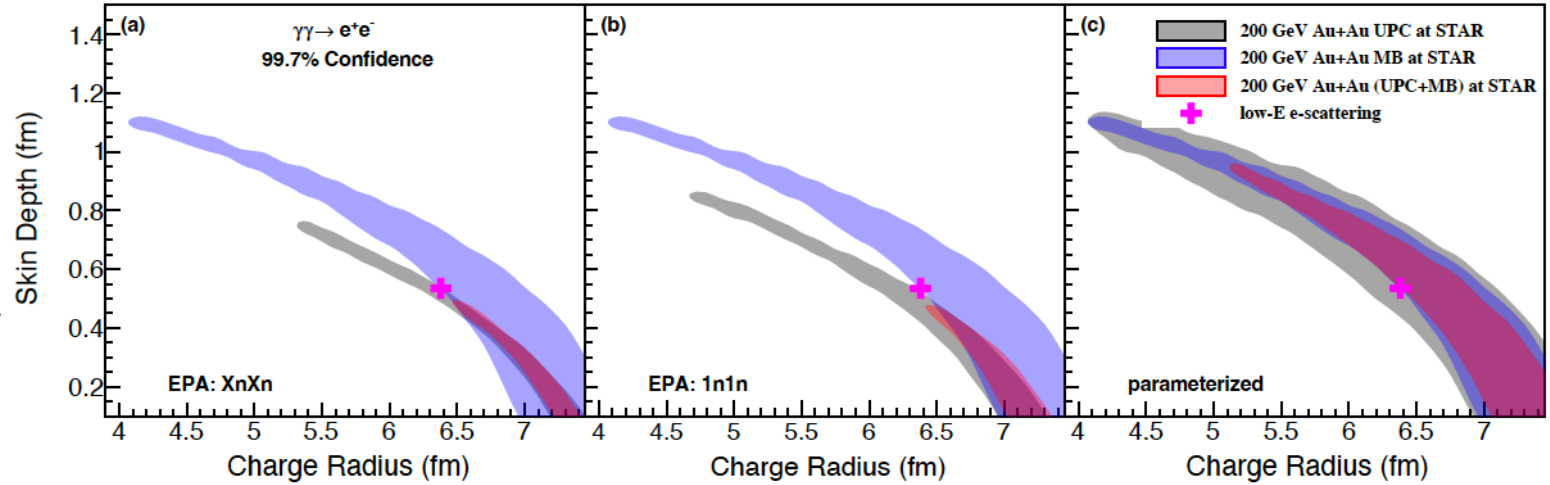


FIG. 5. (color online) The constraints on gold nuclear charge distribution obtained by the comparison of $\gamma\gamma \rightarrow e^+e^-$ and the lowest order QED calculation for different neutron selection conditions in ZDC and parameterized probability. A default $\sigma_{NN} = 41.6$ mb has been used in all other calculations. These are to be compared to the default value of nuclear charge radius RMS of $\sqrt{\langle r^2 \rangle} = 5.33$ fm at $R = 6.38$ fm and $d = 0.535$ fm.

TABLE I. RMS of radius ($\sqrt{\langle r^2 \rangle}$) at minimum χ^2 (χ_{min}^2) and uncertainties within $\chi_{min}^2 + 1$ with different σ_{NN} and with different neutron selection conditions in ZDC and parameterized probability. A default $\sigma_{NN} = 41.6$ mb has been used in all other calculations. These are to be compared to the default value of nuclear charge radius RMS of $\sqrt{\langle r^2 \rangle} = 5.33$ fm at $R = 6.38$ fm and $d = 0.535$ fm.

condition	σ_{NN} (mb)	UPC	MB	UPC+MB
1n1n	35.0	5.55 + 0.03 - 0.30	5.66 + 0.09 - 0.12	5.55 + 0.03 - 0.03
	40.0	5.32 + 0.26 - 0.21	5.67 + 0.08 - 0.10	5.58 + 0.01 - 0.04
	41.6	5.39 + 0.14 - 0.21	5.67 + 0.08 - 0.12	5.53 + 0.10 - 0.02
	45.0	5.47 + 0.02 - 0.21	5.66 + 0.09 - 0.11	5.54 + 0.08 - 0.03
XnXn	35.0	5.70 + 0.01 - 0.29	5.66 + 0.09 - 0.12	5.64 + 0.07 - 0.07
	40.0	5.70 + 0.01 - 0.30	5.67 + 0.08 - 0.10	5.70 + 0.01 - 0.12
	41.6	5.67 + 0.03 - 0.17	5.67 + 0.08 - 0.12	5.67 + 0.03 - 0.09
	45.0	5.54 + 0.17 - 0.16	5.66 + 0.09 - 0.11	5.64 + 0.06 - 0.11
Parameterized	35.0	5.51 + 0.15 - 0.18	5.66 + 0.09 - 0.12	5.61 + 0.13 - 0.11
	40.0	5.43 + 0.22 - 0.08	5.67 + 0.08 - 0.10	5.67 + 0.04 - 0.16
	41.6	5.41 + 0.25 - 0.09	5.67 + 0.08 - 0.12	5.62 + 0.12 - 0.11
	45.0	5.40 + 0.23 - 0.17	5.66 + 0.09 - 0.11	5.62 + 0.09 - 0.11

X.F. Wang, arXiv:2207.05595

Energy-dependence measurements sensitive to the infrared-divergence term

- QED has a well-known infrared-divergence due to the massless of photons ($1/q^4$)
In e+e- collisions, the interaction can be formulated as photon collisions with finite momentum transfer (virtuality) cutoff: q_{\min} and q_{\max} since $\gamma \rightarrow \infty$
(particle data group 2020, section 50.7 Eq.50.44)

- Heavy-ion UPC at RHIC naturally regulated by the form factor at high q and finite ω/γ at low q . This is crucial for discovery of the Breit-Wheeler process and the photon spatial-momentum-spin correlation
Vector direction and resolving power become poor as $q \rightarrow 0$

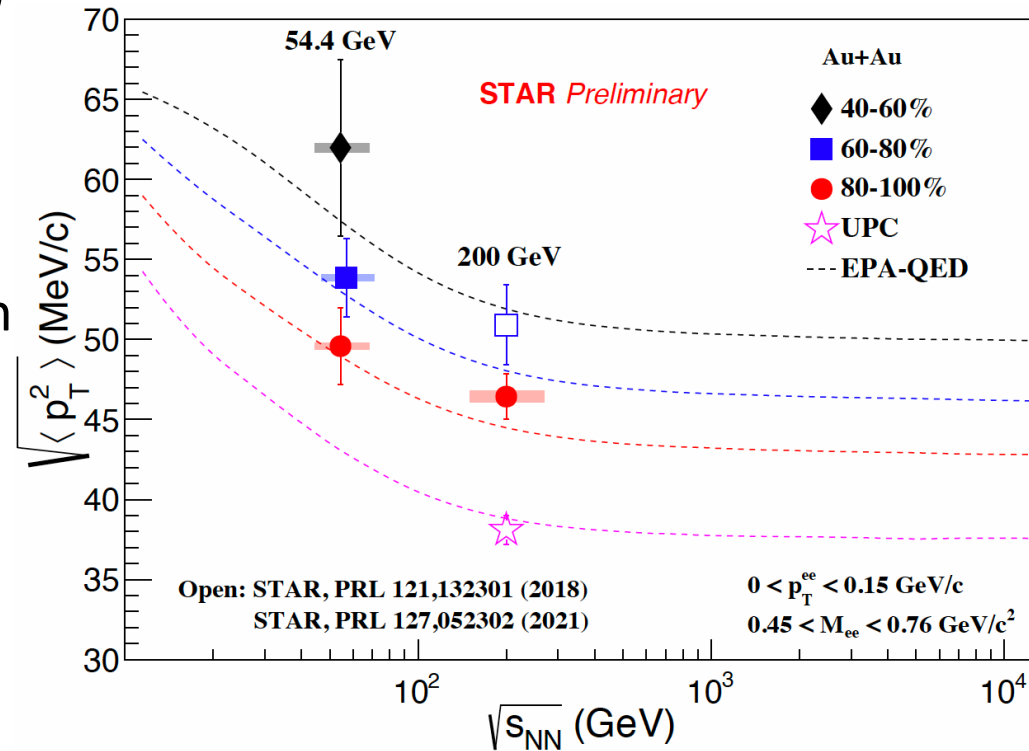
- We can further test this by studying the beam energy (γ) dependence of $\langle p_t \rangle$. Analytic integration:

$$\langle p_t^2 \rangle = \int_0^\infty p_t^2 dn \approx (\hbar/R)^2 - 4 \left(\frac{\omega}{\gamma}\right)^2 \ln\left(\frac{R\omega}{\gamma}\right)$$

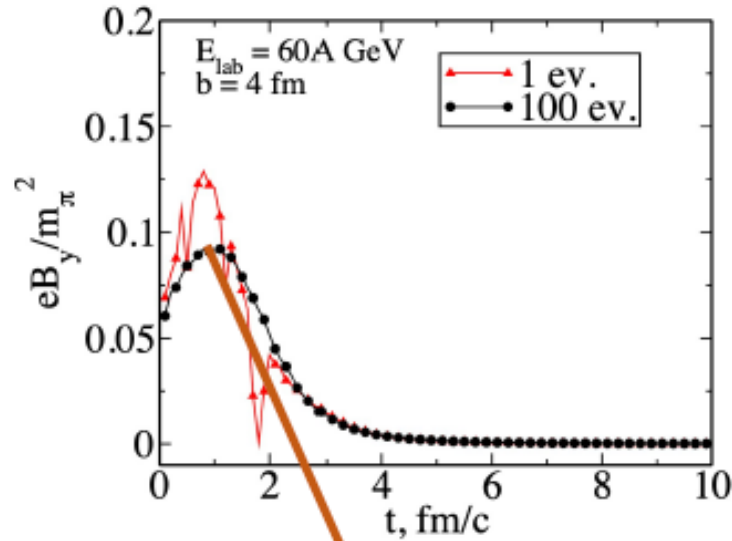
For $\omega=300\text{MeV}$, $R=6.8\text{fm}$,

BW $\langle p_t \rangle \approx 41\text{MeV}$ at $\gamma \rightarrow \infty$, 44MeV at $\gamma=100$, 53MeV at $\gamma=25$;

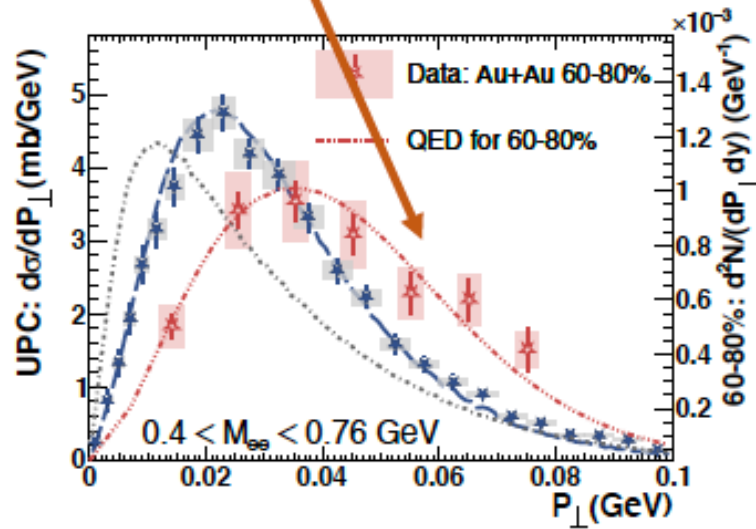
$$dn_i = \frac{Z_i^2 \alpha q_{i\perp}^2 \left[F \left(q_{i\perp}^2 + \frac{w_i^2}{\gamma^2} \right) \right]^2 d^3 q_i}{\pi^2 \left(q_{i\perp}^2 + \frac{w_i^2}{\gamma^2} \right)^2 w_i}$$



Event-by-event Fluctuations + Interactions



- Significantly stronger field possible at small radial distances (based on current data)
- Fluctuating nucleon positions effect field inside nucleus
- OR Long-lived magnetic field
→ Lorentz-force bending of pairs
- High precision data from STAR 2023-25
- What to look for:
 - Field at small distance → large P_{\perp} and α
 - Look for modification of $d\sigma/dP_{\perp}$ shape



Hint of modification in 60 – 80% central collisions:
Additional 14 ± 4 (stat.) ± 4 (syst.) MeV/c broadening

Most Precision test in Central Pb+Pb at LHC

- Under what condition do these photons interact as real photons?
 - Photon Wigner Function (PWF) formalism & LO-QED formalism agree very well
 - How to understand the minor differences between them?

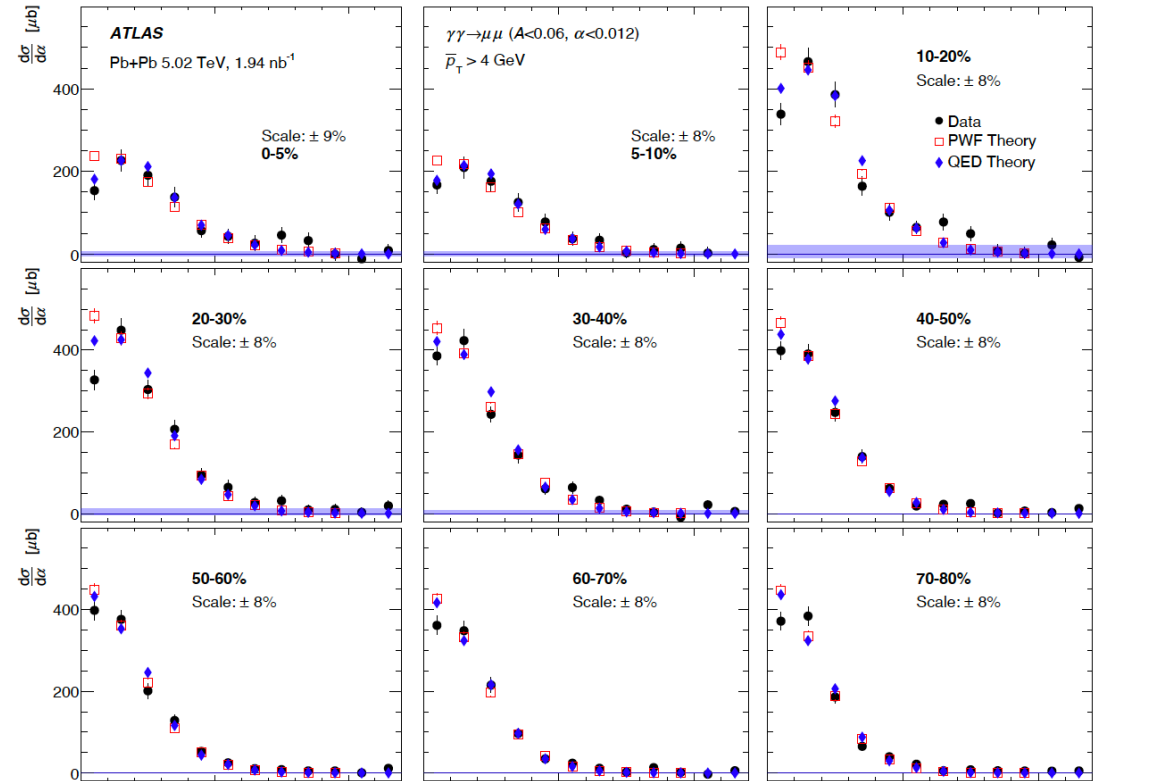
- Possible difference between data and QED due to final-state B-field?

$$\omega/\gamma \lesssim k_{\perp} \lesssim 1/R \ll \omega,$$

$$\frac{\sqrt{2}}{\gamma} \lesssim \frac{\pi}{2} \alpha \lesssim \frac{\sqrt{2}}{\omega R} \ll 1$$

$\Delta\phi$

$$\alpha \equiv 1 - \Delta\phi/\pi$$



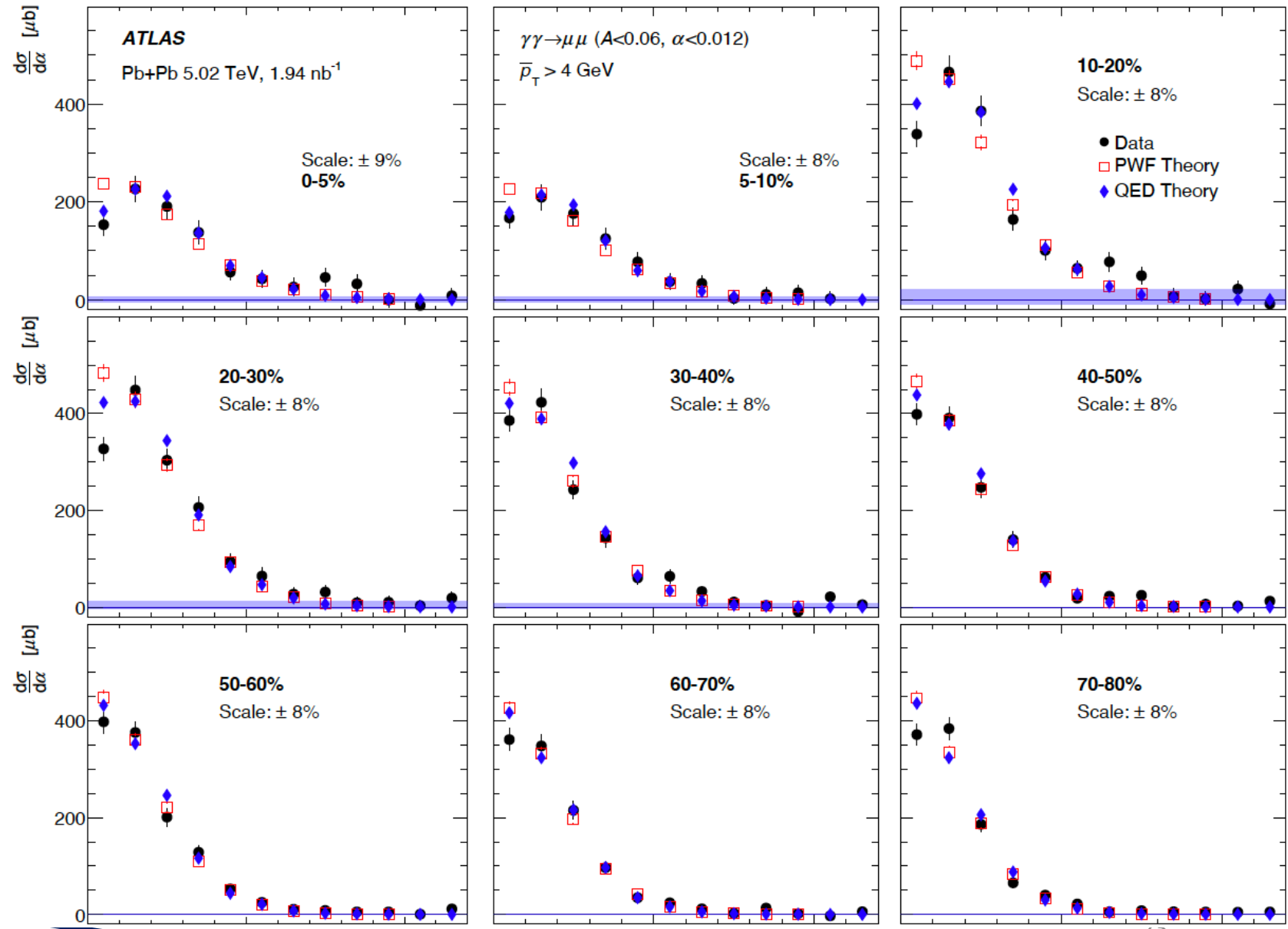
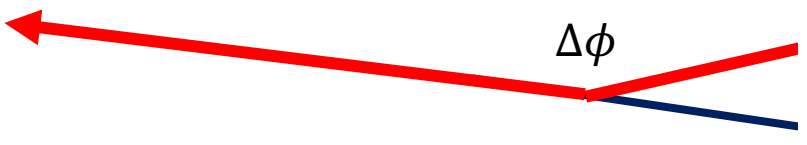
ATLAS, arXiv:2206.12594; PRL 2018

Most Precision test in Central Pb+Pb at LHC

- Under what condition do
 - Photon Wigner Function (formalism & LO-QED form)
 - How to understand the m
 - Possible difference betw and QED due to final-st field?

$$\omega/\gamma \lesssim k_{\perp} \lesssim 1/R \ll \omega,$$

$$\frac{\sqrt{2}}{\gamma} \lesssim \frac{\pi}{2} \alpha \lesssim \frac{\sqrt{2}}{\omega R} \ll 1$$



ATLAS, arXiv:2206.12594; PRL 2018

Are there final-state QED effects?

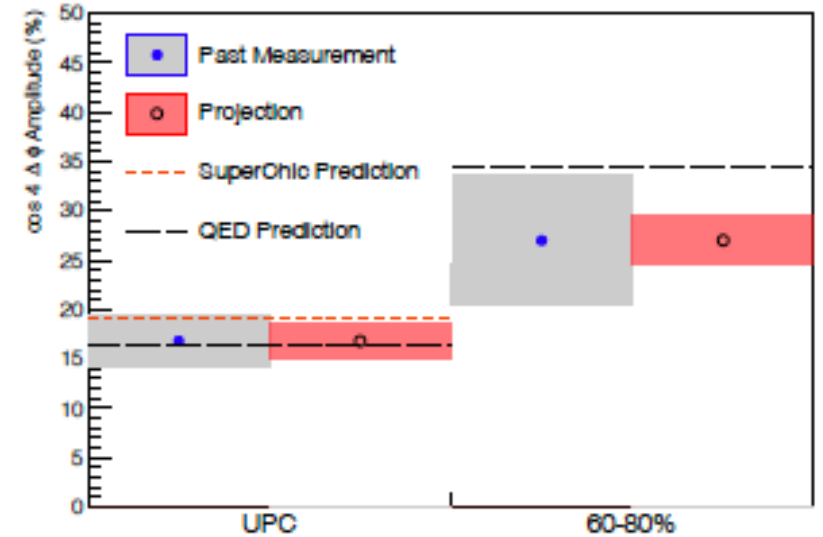
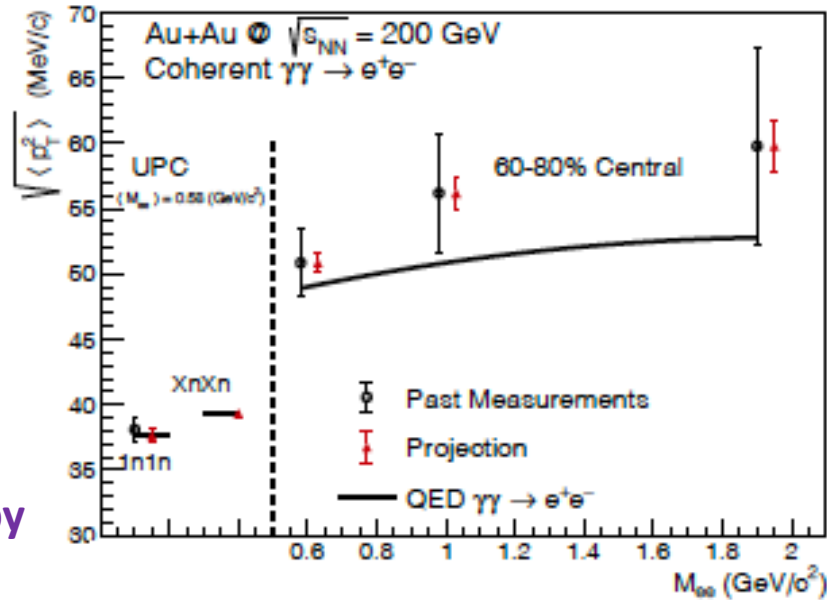


Figure 57: (Color online) Projections for measurements of the $\gamma\gamma \rightarrow e^+e^-$ process in peripheral and ultra-peripheral collisions. Left: The $\sqrt{\langle p_T^2 \rangle}$ of di-electron pairs within the fiducial acceptance as a function of pair mass, M_{ee} , for 60–80% central and ultra-peripheral Au+Au collisions at $\sqrt{s_{NN}} = 200$ GeV. Right: The projection of the $\cos 4\Delta\phi$ measurement for both peripheral (60–80%) and ultra-peripheral collisions.

STAR Beam Use Request (2023-2025):

https://drupal.star.bnl.gov/STAR/system/files/BUR2020_final.pdf

p_T broadening and azimuthal correlations of e^+e^- pairs sensitive to electro-magnetic (EM) field;

Impact parameter dependence of transverse momentum distribution of EM production is the key component to describe data.

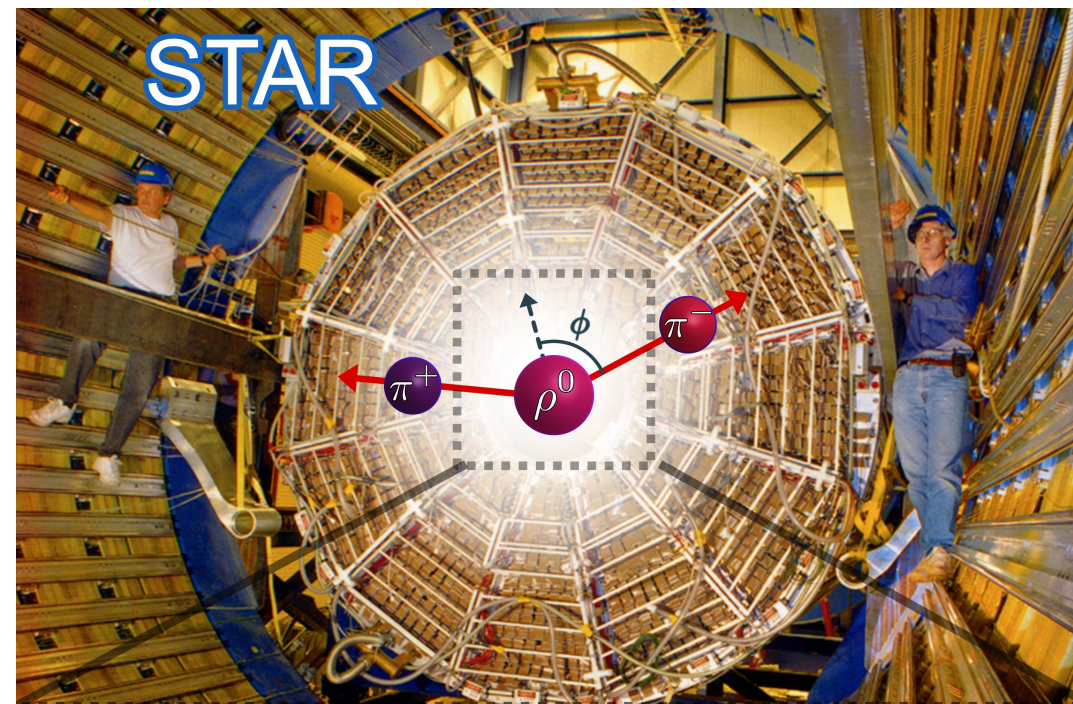
Is there a sensitivity to final magnetic field in QGP?

Precise measurement of p_T broadening and angular correlation will tell at $>3\sigma$ for each observable.

Spin Interference Enabled Nuclear Tomography

STAR, arXiv:2204.01625

- Teaser:
Polarized photon-gluon fusion reveals quantum wave interference of non-identical particles and shape of high-energy nuclei

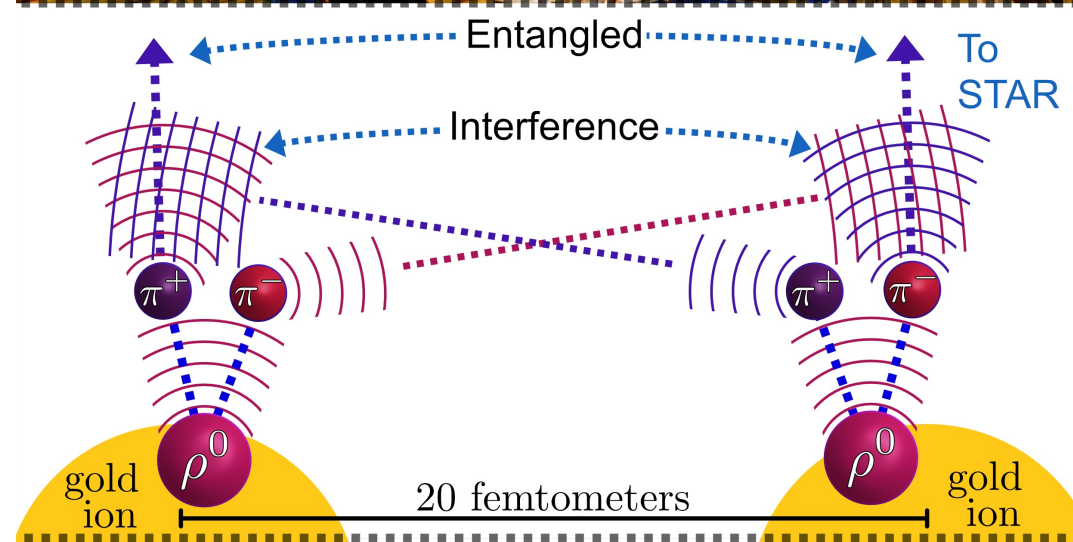
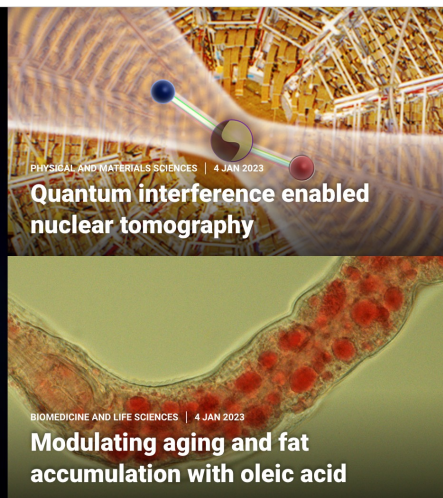
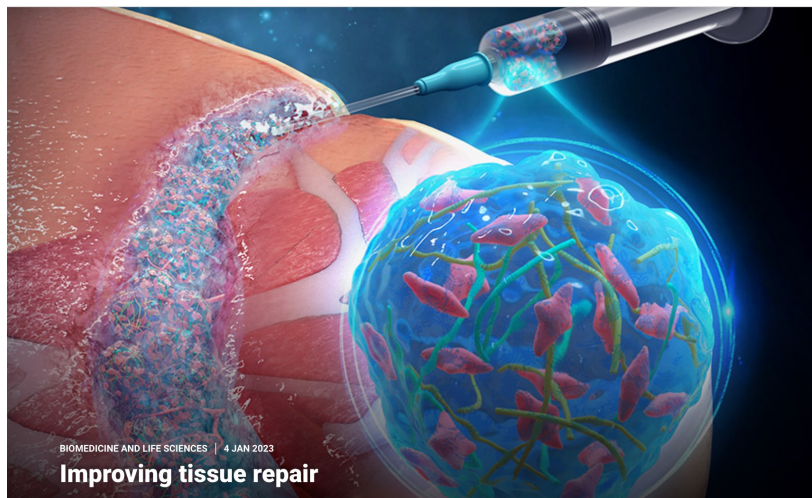


ScienceAdvances

Current Issue First release papers Archive About

Submit manuscript

GET OUR E-ALERTS

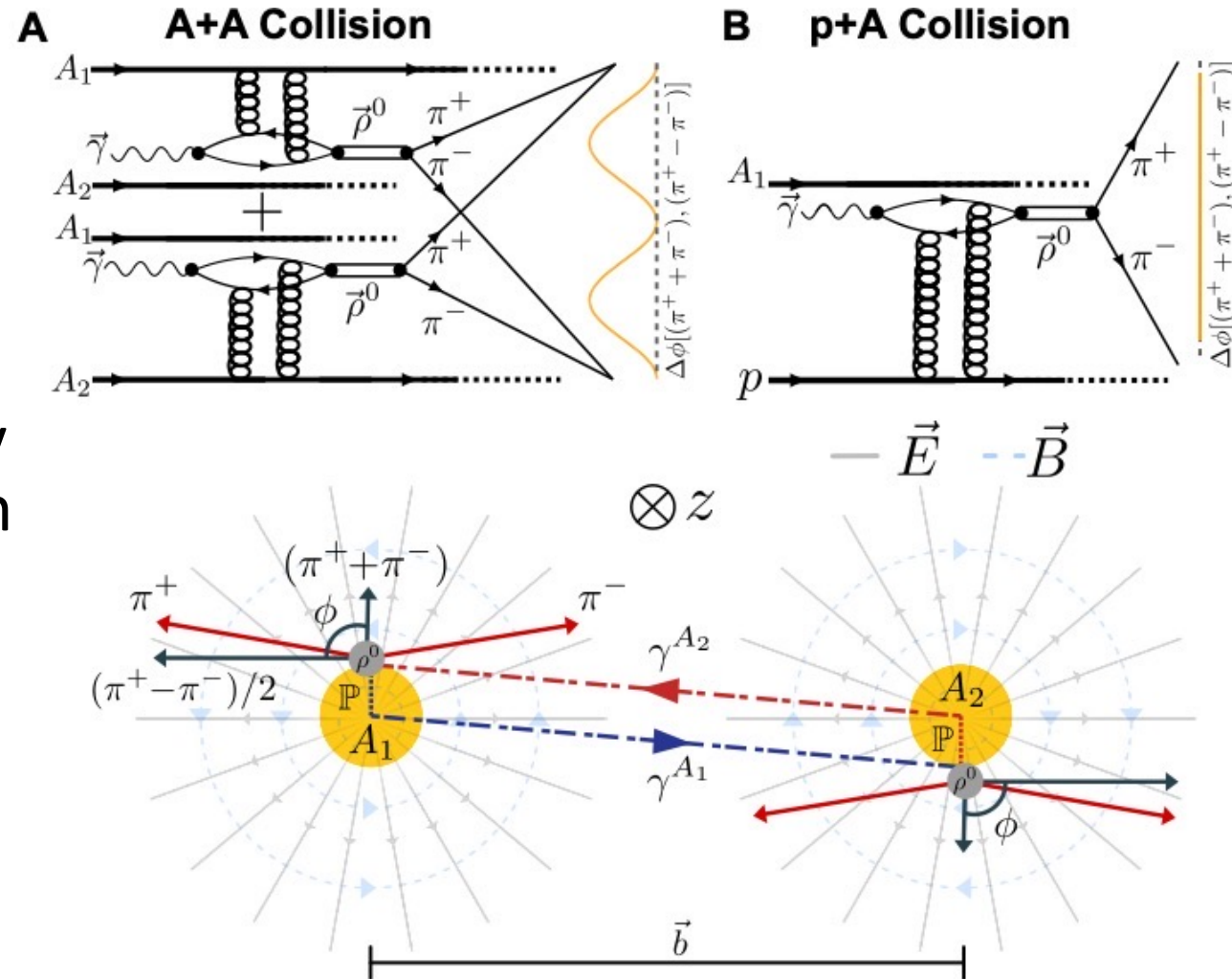


Three Ingredients

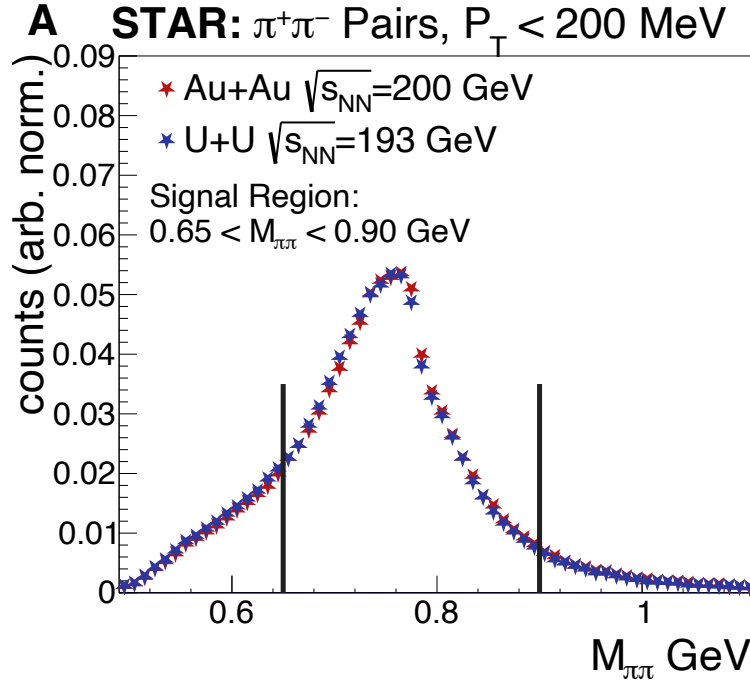
- Linearly Polarized photoproduction of vector meson
- At a distance with two wavefunctions (180° rotation symmetry)
- Entanglement between π^\pm from ρ decay and interference between identical pion wavefunction

IF I have said that this is what reality is without any experimental evidence, most people would have thought that I am crazy.

“Truth is Stranger than Fiction,
but it is because Fiction is obligated
to stick to possibilities; Truth isn’t.”
– Mark Twain



$\Delta\phi$ in Au+Au and U+U Collisions



Quantify the difference in strength for Au+Au vs. U+U via a fit:

$$f(\Delta\phi) = 1 + a \cos 2\Delta\phi$$

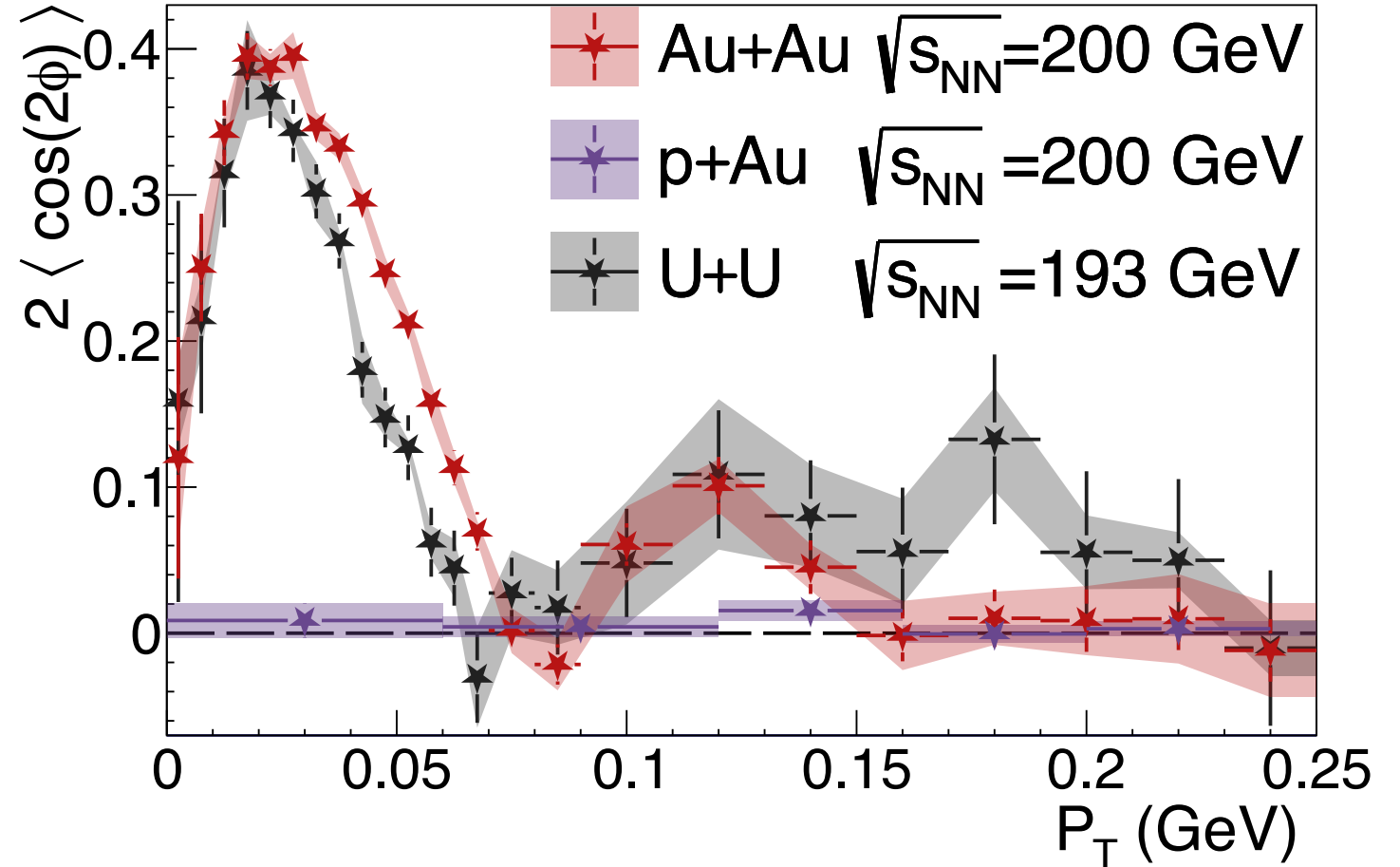
Au+Au : $a = 0.292 \pm 0.004$ (stat) ± 0.004 (syst.)

U+U : $a = 0.237 \pm 0.006$ (stat) ± 0.004 (syst.)

Difference of 4.3 σ (stat. & syst.):

[arXiv:2204.01625](https://arxiv.org/abs/2204.01625)

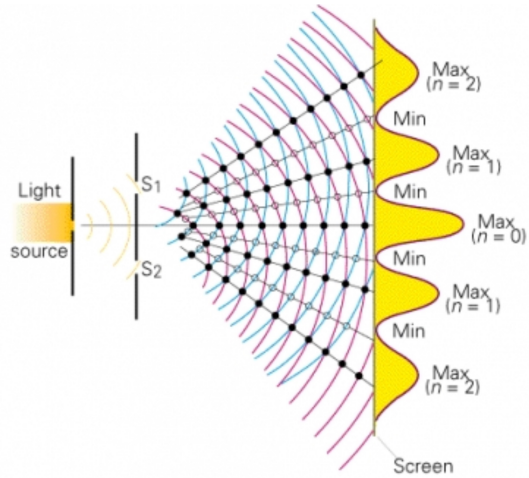
B STAR: Signal $\pi^+\pi^-$ pairs



- Interference effect is sensitive to the nuclear geometry (gluon distribution) – difference between Au and U

Novel Form of Quantum Interference

Similar to double-slit experiment

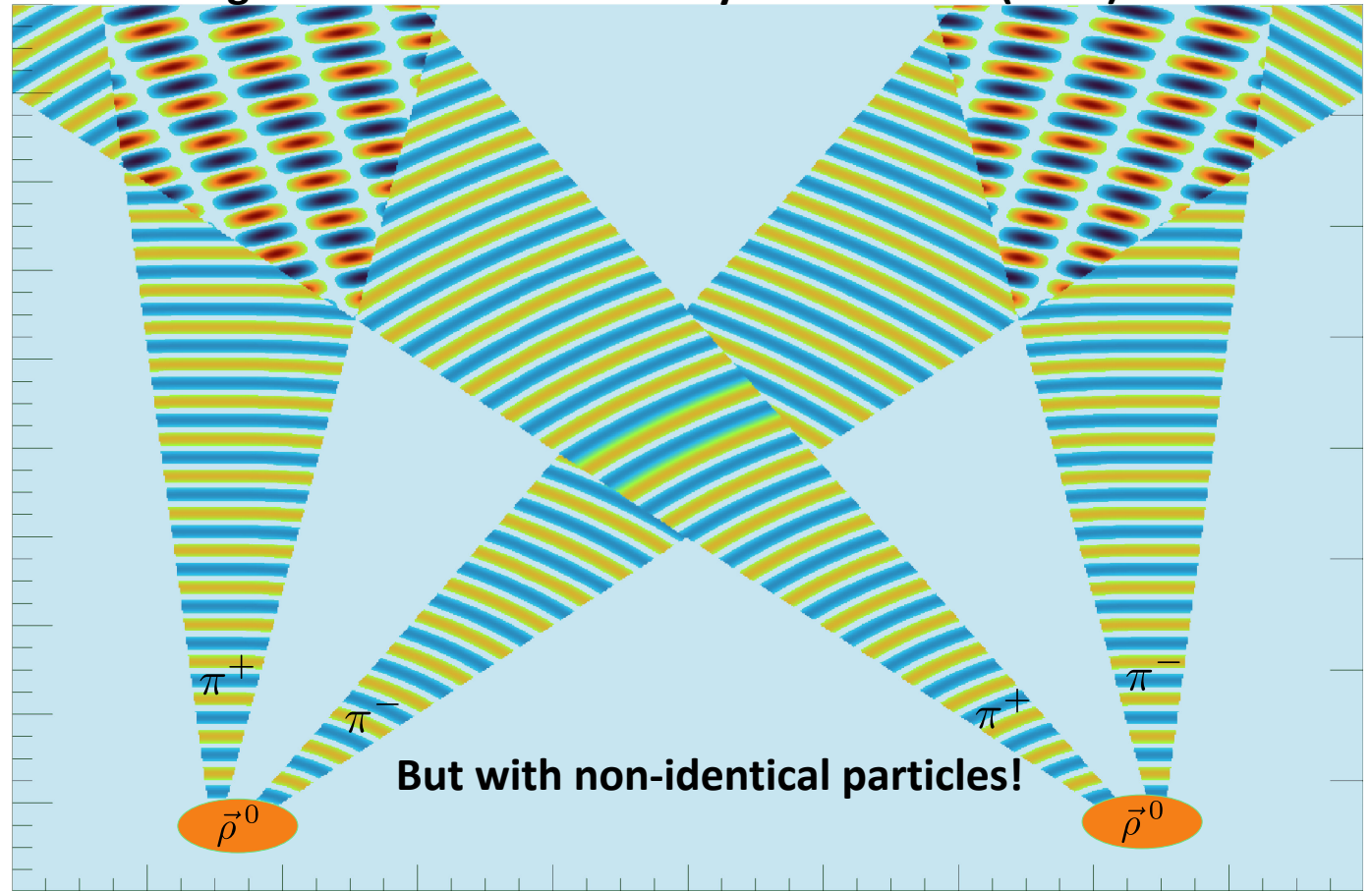


BUT

Interference occurs between **distinguishable** particles



Entanglement Enabled Intensity Interference ($E^2 I^2$)



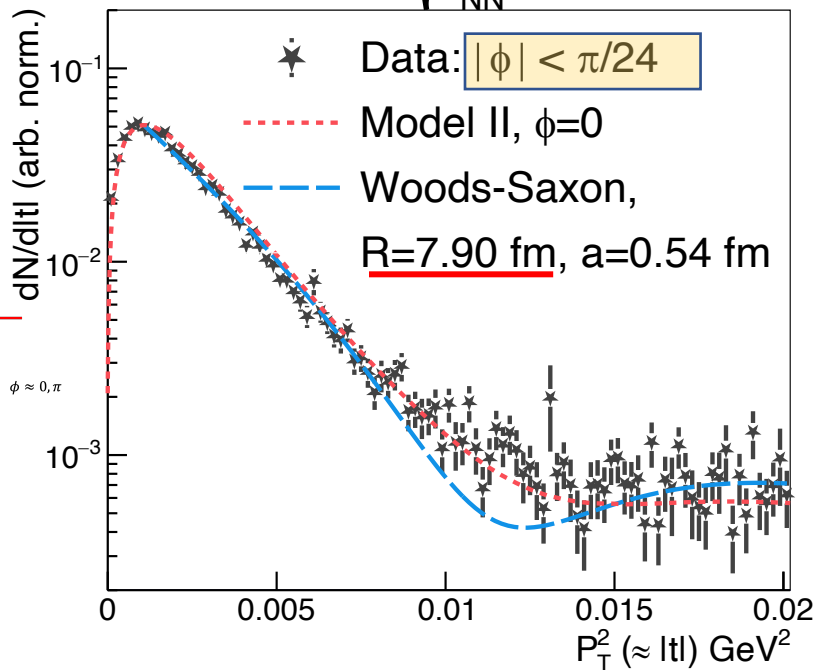
Possible theoretical explanation from Frank Wilczek's group at MIT – Entanglement enabled interference of amplitudes from non-identical particles

J. Cotler, F. Wilczek, and V. Borish, *Annals of Physics* **424**, 168346 (2021).

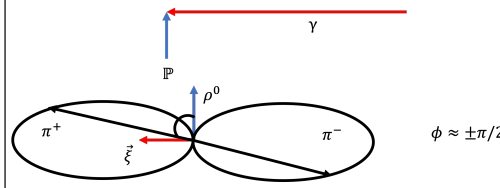
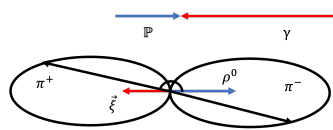
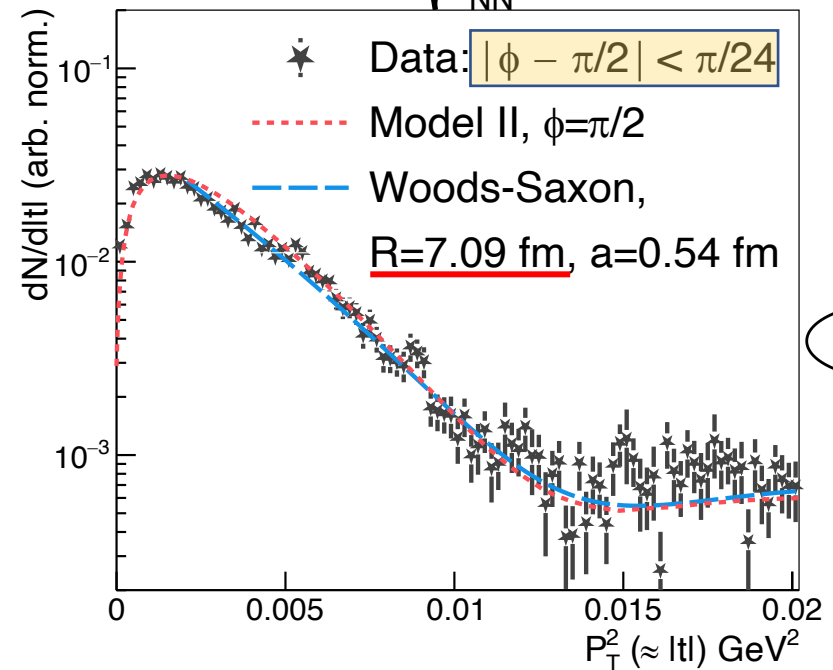
$|t|$ vs. ϕ , which radius is 'correct'?

Now instead of p_x and p_y lets look at $|t|$ with a 2D approach

STAR: Au+Au $\sqrt{s_{NN}}=200$ GeV



STAR: Au+Au $\sqrt{s_{NN}}=200$ GeV



- Drastically different radius depending on ϕ , still way too big
- Notice how much better the Woods-Saxon dip is resolved for $\phi = \pi/2$ -> experimentally able to **remove photon momentum, which blurs diffraction pattern**

[arXiv:2204.01625](https://arxiv.org/abs/2204.01625)

Can we extract the 'true' nuclear radius from $|t|$ vs. ϕ information?

Precision radius measurement with interference

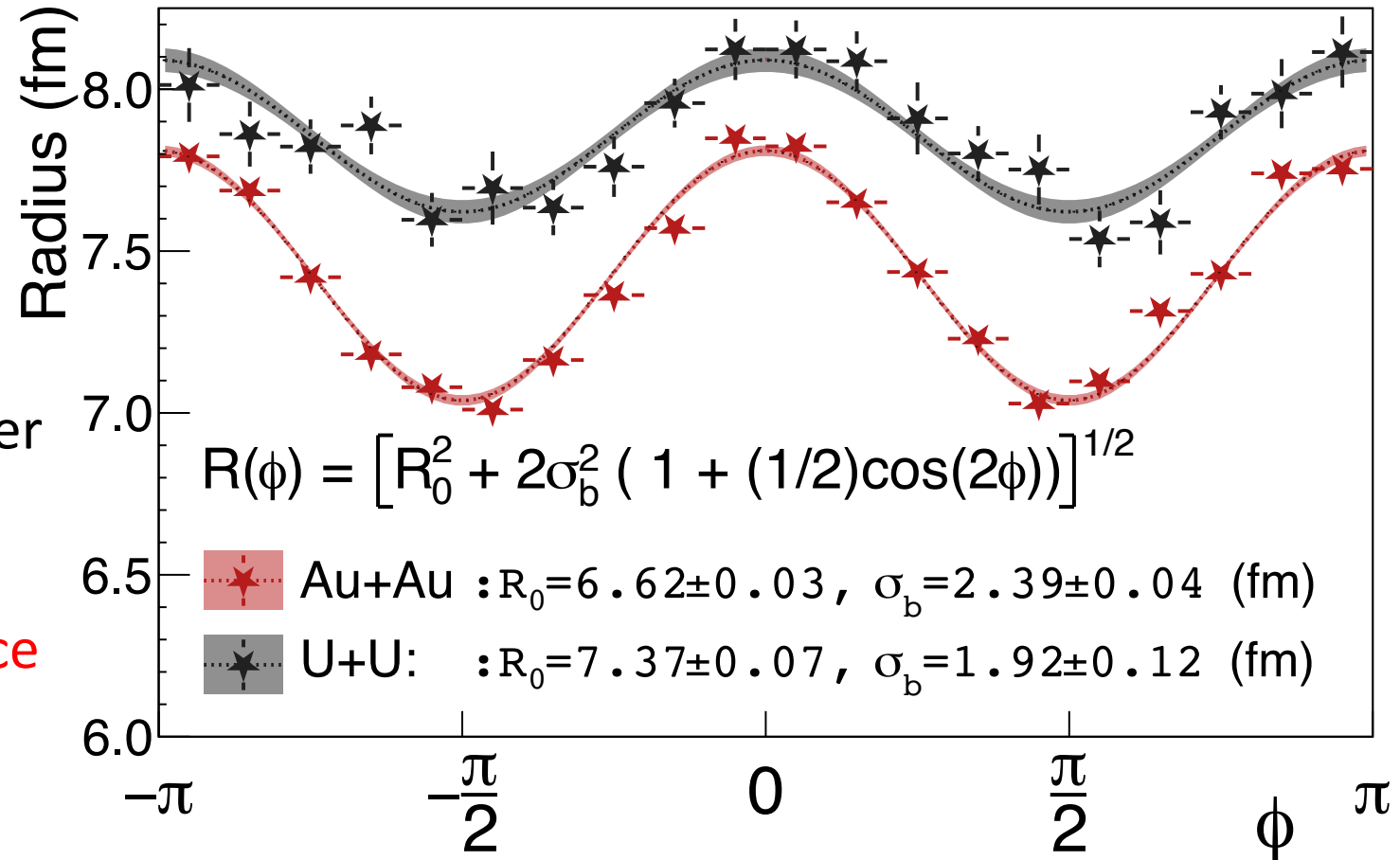
STAR, arXiv:2204.01625

STAR: Photonuclear $\rho^0 \rightarrow \pi^+\pi^-$

Azimuthal variation due to:

- Photon linear polarization,
- Spin transfer to VM
- Photon finite k_T
- VM spin 1 decay to spin 0 pions
- Interference along impact parameter

These image blurring effects can be improved with the angular dependence



Extracted neutron skins and comparison to world data

	Au+Au (fm)	U+U (fm)
Charge Radius	6.38 (long: 6.58, short: 6.05)	6.81 (long: 8.01, short: 6.23)
Inclusive t slope (STAR 2017) [1]	7.95 ± 0.03	--
Inclusive t slope (WSFF fit)*	7.47 ± 0.03	7.98 ± 0.03
Tomographic technique*	6.53 ± 0.03 (stat.) ± 0.05 (syst.)	7.29 ± 0.06 (stat.) ± 0.05 (syst.)
DESY [2]	6.45 ± 0.27	6.90 ± 0.14
Cornell [3]	6.74 ± 0.06	--
Neutron Skin (Tomographic Technique)*	0.17 ± 0.03 (stat.) ± 0.08 (syst.) $\sim 2\sigma$	0.44 ± 0.05 (stat.) ± 0.08 (syst.) $\sim 4.7\sigma$ (Note: for Pb ≈ 0.3)

M. Centelles, X. Roca-Maza, X. Viñas, and M. Warda
Phys. Rev. Lett. **102**, (2009) 122502

GIULIANO GIACALONE, July 22, 2022

$$\Delta r_{np} = 0.283 \pm 0.071 \text{ fm}$$

$$L = (106 \pm 37) \text{ MeV}$$

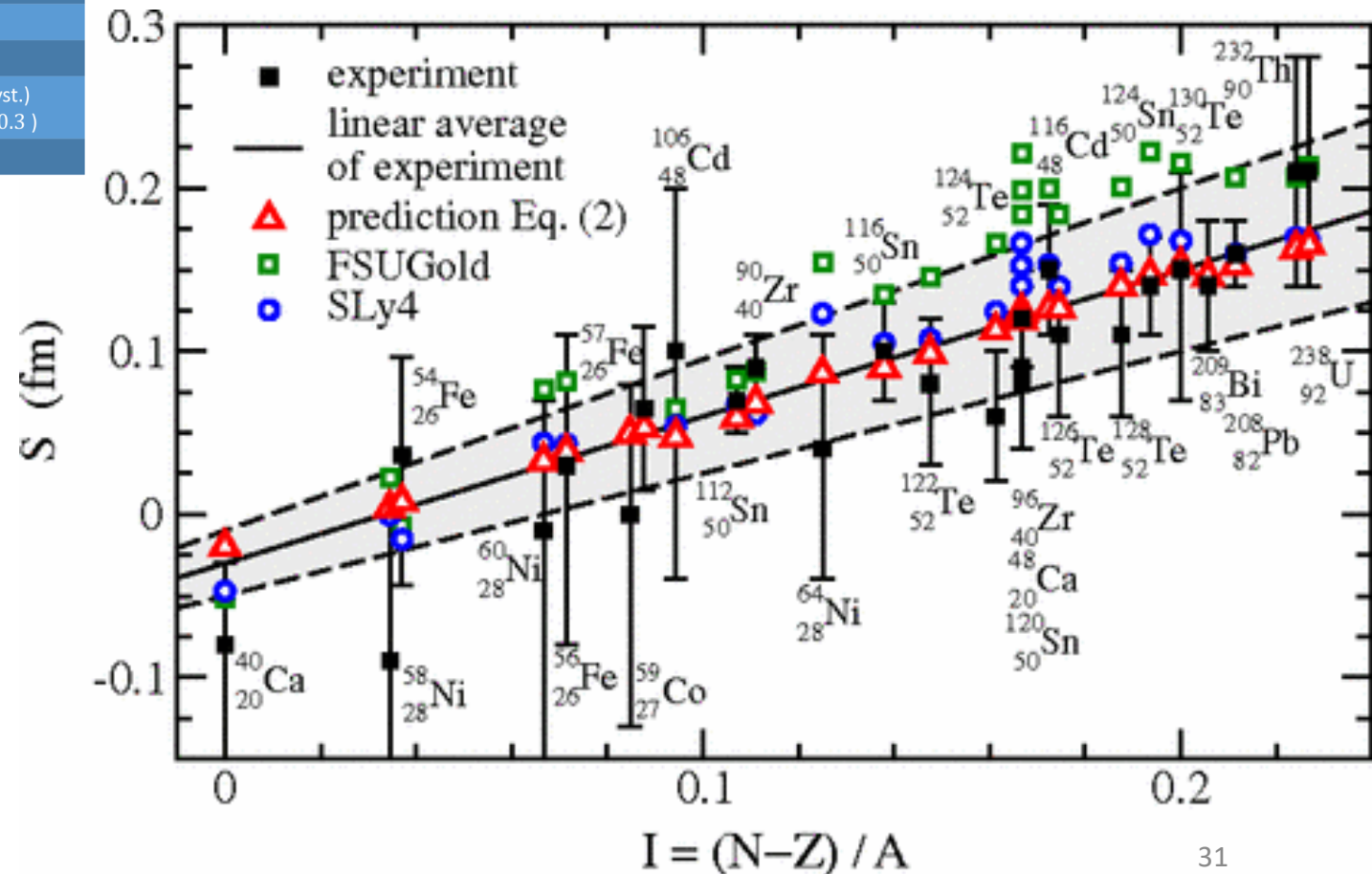
[PREX-II experiment,
PRL **126** (2021) 17, 172502]

Stiffer EoS than expected.

[Reed et al., PRL **126** (2021) 17, 172503]
[Fattoyev et al., PRL **120** (2018) 17, 172702]

From
GW170817

of $\Lambda_{1,4} \lesssim 580$ [44], we eagerly await the next generation of terrestrial experiments and astronomical observations to verify whether the tension remains. If so, the softening of the EOS at intermediate densities, together with the subsequent stiffening at high densities required to support massive neutron stars, may be indicative of a phase transition in the stellar core [42].



Can we get an independent estimate at RHIC?

Extracted neutron skins and comparison to world data

	Au+Au (fm)	U+U (fm)
Charge Radius	6.38 (long: 6.58, short: 6.05)	6.81 (long: 8.01, short: 6.23)
Inclusive t slope (STAR 2017) [1]	7.95 ± 0.03	--
Inclusive t slope (WSFF fit)*	7.47 ± 0.03	7.98 ± 0.03
Tomographic technique*	6.53 ± 0.03 (stat.) ± 0.05 (syst.)	7.29 ± 0.06 (stat.) ± 0.05 (syst.)
DESY [2]	6.45 ± 0.27	6.90 ± 0.14
Cornell [3]	6.74 ± 0.06	--
Neutron Skin (Tomographic Technique)*	0.17 ± 0.03 (stat.) ± 0.08 (syst.) $\sim 2\sigma$	0.44 ± 0.05 (stat.) ± 0.08 (syst.) $\sim 4.7\sigma$ (Note: for Pb ≈ 0.3)

M. Centelles, X. Roca-Maza, X. Viñas, and M. Warda
Phys. Rev. Lett. **102**, (2009) 122502



GIULIANO GIACALONE, July 22, 2022

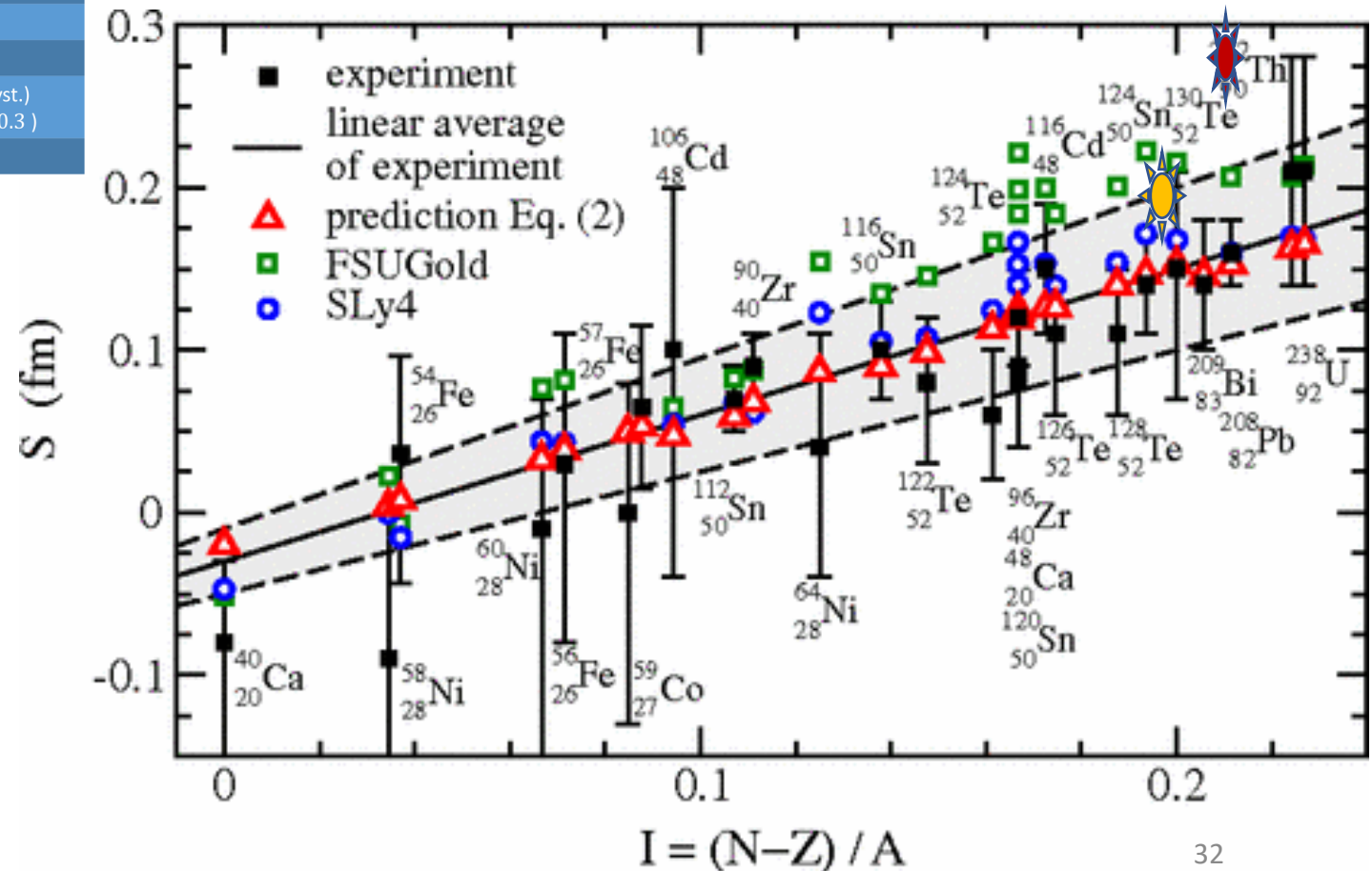
$$\Delta r_{np} = 0.283 \pm 0.071 \text{ fm}$$

$$L = (106 \pm 37) \text{ MeV}$$

[PREX-II experiment,
PRL **126** (2021) 17, 172502]

Stiffer EoS than expected. [Reed et al., PRL **126** (2021) 17, 172503]
[Fattoyev et al., PRL **120** (2018) 17, 172702]

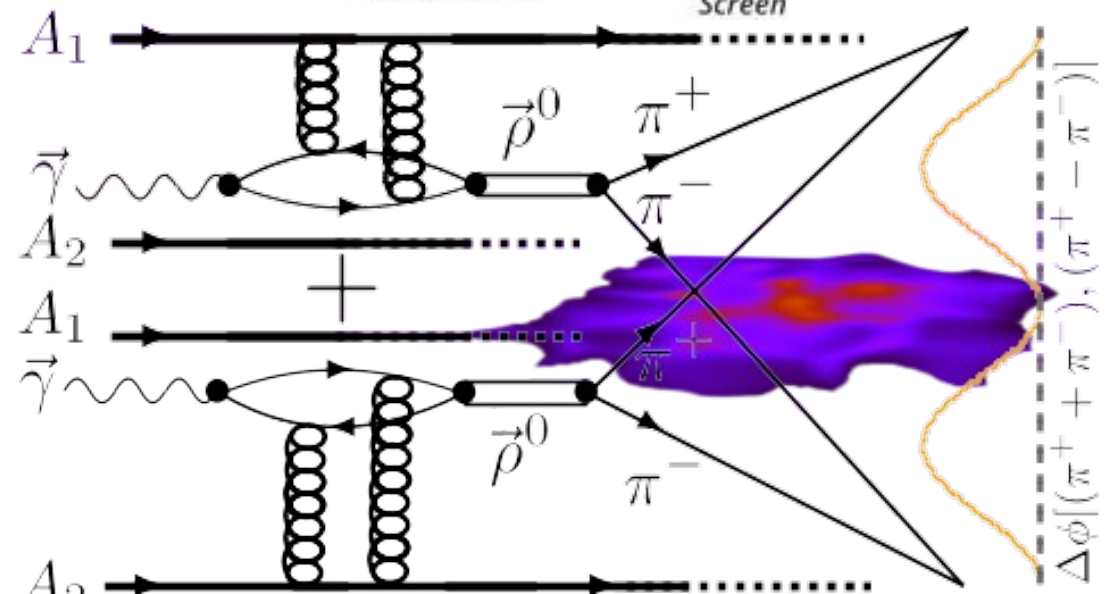
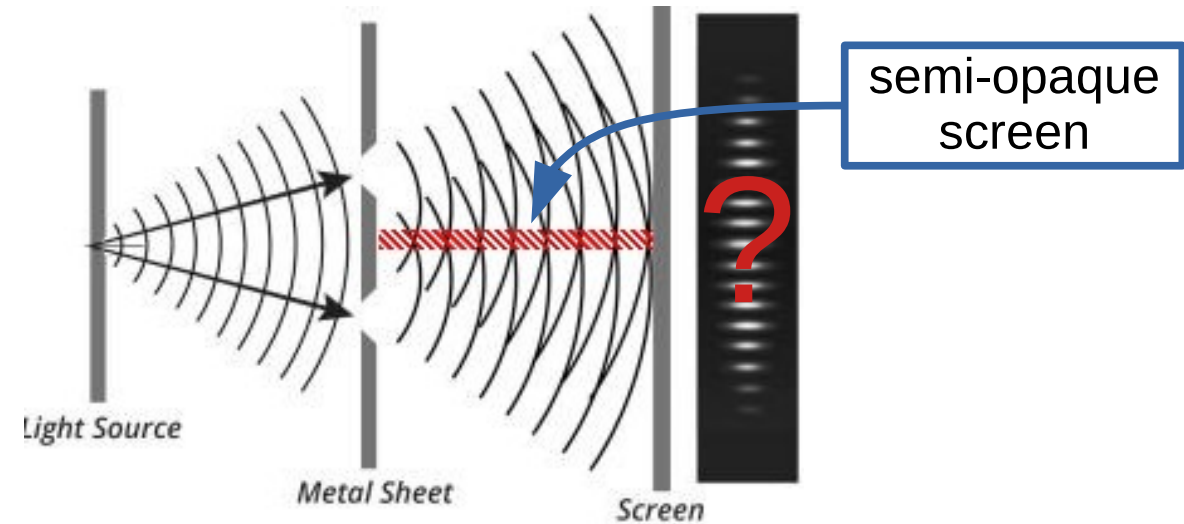
From GW170817 \rightarrow of $\Lambda_{1,4} \lesssim 580$ [44], we eagerly await the next generation of terrestrial experiments and astronomical observations to verify whether the tension remains. If so, the softening of the EOS at intermediate densities, together with the subsequent stiffening at high densities required to support massive neutron stars, may be indicative of a phase transition in the stellar core [42].



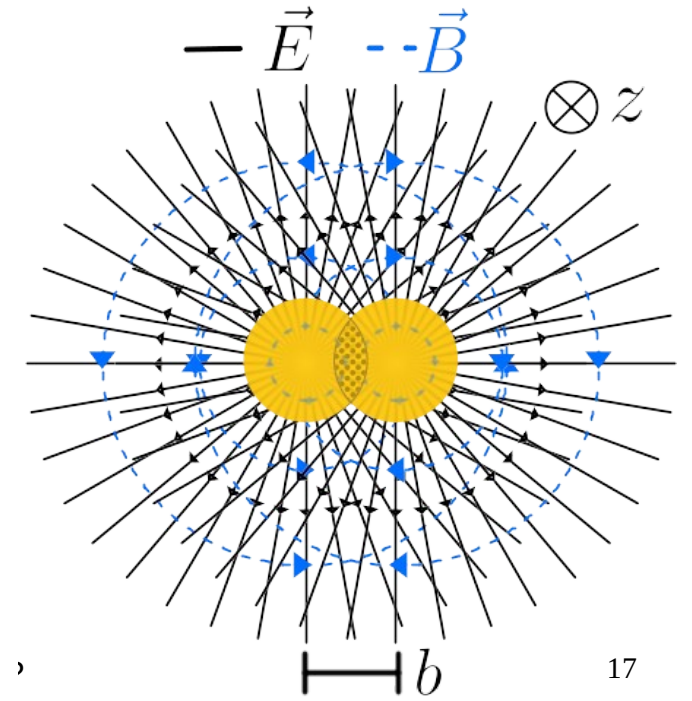
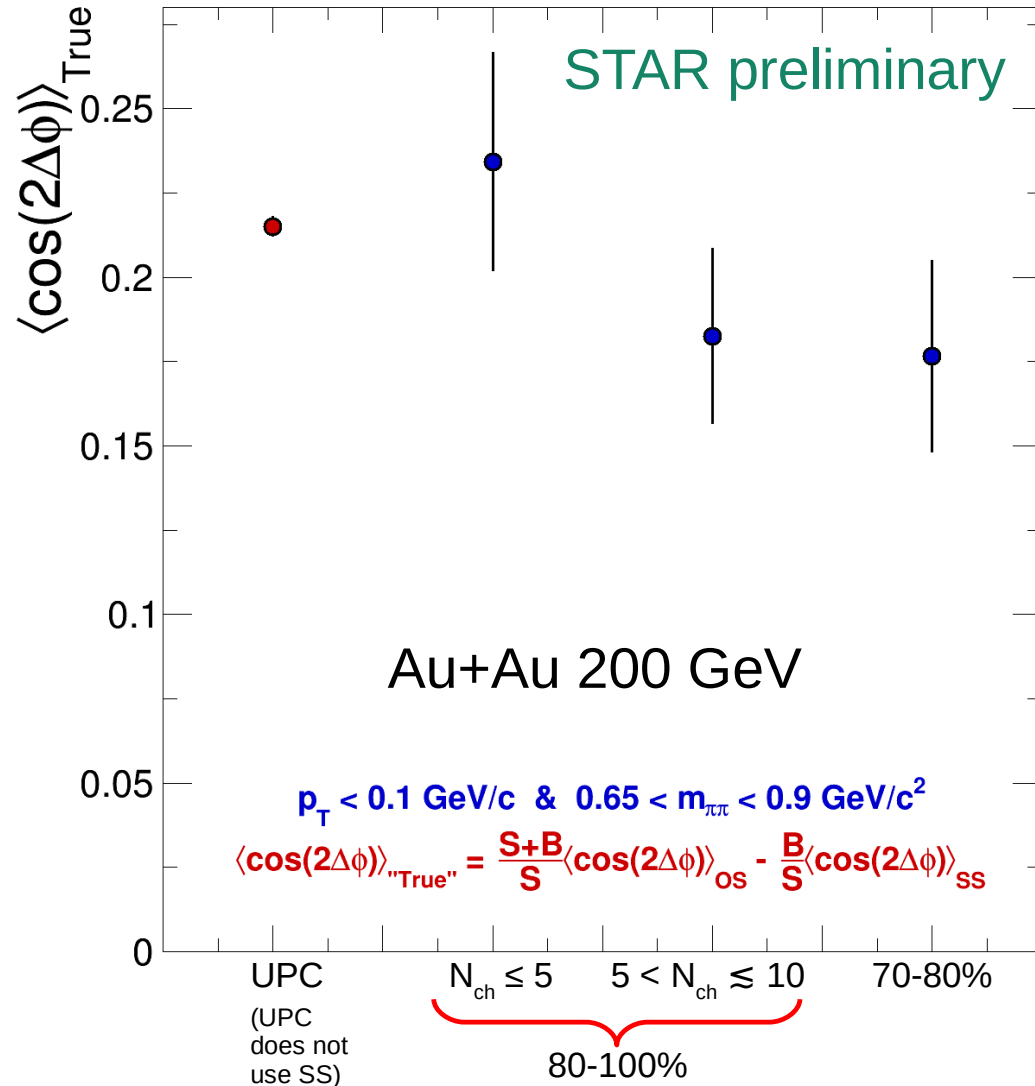
Can we get an independent estimate at RHIC?

Modification of double-slit

- In double-slit analogy hadronic interactions might be semi-opaque screen dividing the holes
- J/ψ measurements demonstrate coherent photoproduction in central collisions, but do not investigate how these hadronic interactions affect the wave function



The magic of spin alignment in photoproduction



The alignments along impact-parameter cancel

The spin alignment becomes along the B-field direction

Analog to Hagedorn temperature vs thermalization:
Where hadrons are born into the available phase space
instead of dynamically achieving thermalization

Global Polarization is required by rotation symmetry
instead of dynamically achieving polarization

Azimuthal asymmetry in coherent J/ψ

[JDB, et. al., arXiv:2207.02478](#) [hep-ph]

Can resolve whether the polarization is from initial or final states

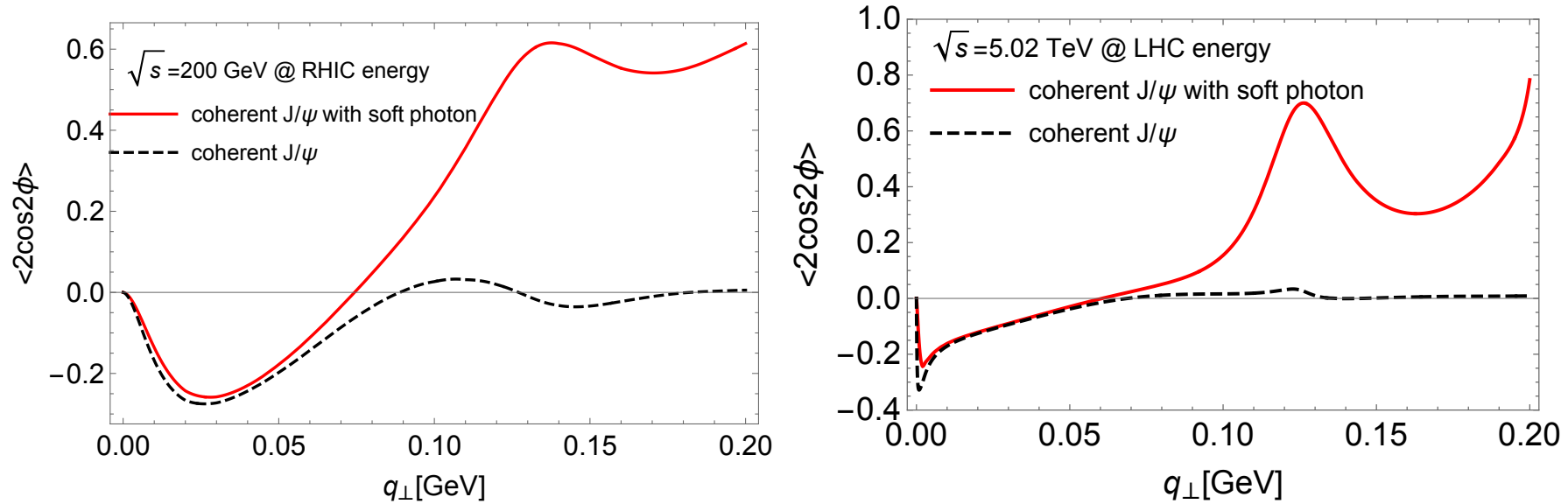


FIG. 3: $\cos 2\phi$ azimuthal asymmetry in coherent J/ψ production at RHIC energy and LHC energy. The rapidity of the di-lepton pair is integrated over the range $[-1, 1]$ at RHIC kinematics and $[-0.8, 0.8]$ at LHC kinematics. J/ψ is reconstructed via the decay mode $J/\psi \rightarrow e^+e^-$ at RHIC and $J/\psi \rightarrow \mu^+\mu^-$ at LHC, respectively.

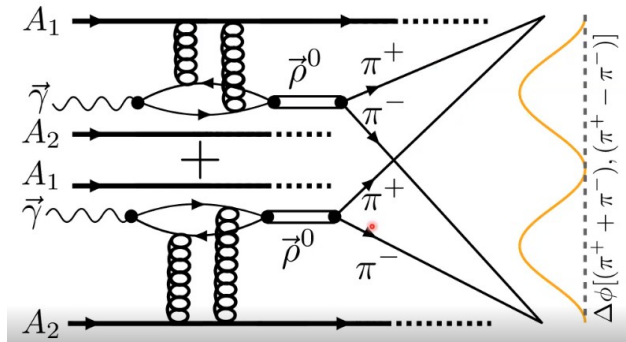
Summary and Perspectives

- Precise QED calculations and matching experimental data with high statistics from initial photon collisions
- Possible systematical deviation in peripheral at RHIC and central collisions at LHC due to final-state B-field effect
- New EM field and polarization effect in photoproduction, connection to global alignment?
- Model: QED+final-state B-field to match data
- RHIC data with more central collisions and high statistics (2023-2025)
- Photoproduction J/Psi and polarization effect in non-UPC A+A collisions

Precise Nuclear Tomography

Neutron skin physics at RHIC.

Ultra-peripheral collisions.



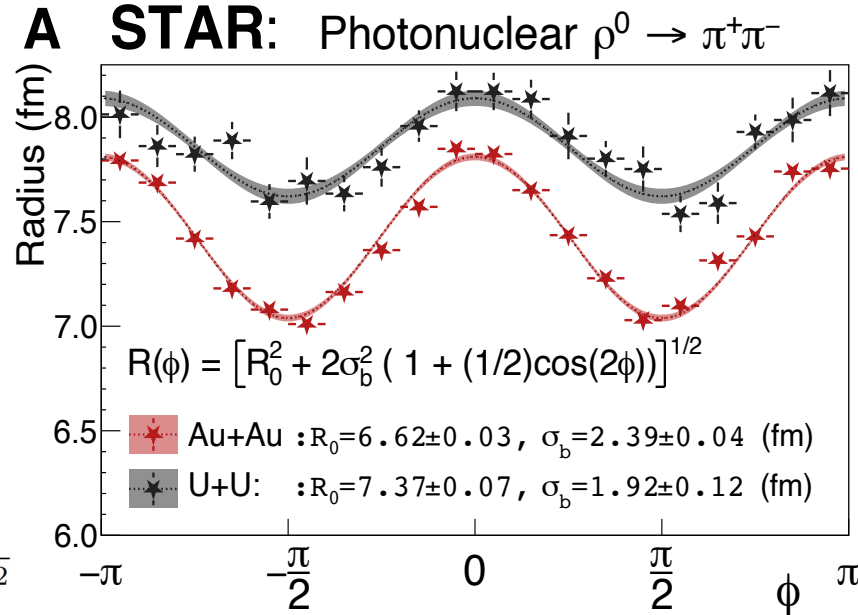
$$f(t) = A_c \mathcal{F}[\rho_A(r; R, a)] (|t|)^2 + \frac{A_i/Q_0^2}{(1 + |t|/Q_0^2)^2}$$

FT of gluon density
(Woods-Saxon)

neutron skins:

$$0.44 \pm 0.05(\text{stat.}) \pm 0.08(\text{syst.}) \text{ fm for } ^{238}\text{U}$$

$$0.17 \pm 0.03(\text{stat.}) \pm 0.08(\text{syst.}) \text{ fm for } ^{197}\text{Au}$$



[STAR Collaboration, arXiv:2204.01625]

Neutron skin physics at RHIC.

The neutron skin in atomic nuclei, Δr_{np} , is proportional to the slope L of symmetry energy.

Accurate measurement of Δr_{np} of ^{208}Pb from neutral weak form factor at JLab (PREX-II experiment):

$$\Delta r_{np} = 0.283 \pm 0.071 \text{ fm}$$

[PREX-II experiment, PRL 126 (2021) 17, 172502]

$$L = (106 \pm 37) \text{ MeV}$$

Stiffer EoS than expected. [Reed et al., PRL 126 (2021) 17, 172503] [Fattoyev et al., PRL 120 (2018) 17, 172702]

From GW170817

of $A_{1.4} \lesssim 580$ [44], we eagerly await the next generation of terrestrial experiments and astronomical observations to verify whether the tension remains. If so, the softening of the EOS at intermediate densities, together with the subsequent stiffening at high densities required to support massive neutron stars, may be indicative of a phase transition in the stellar core [42].

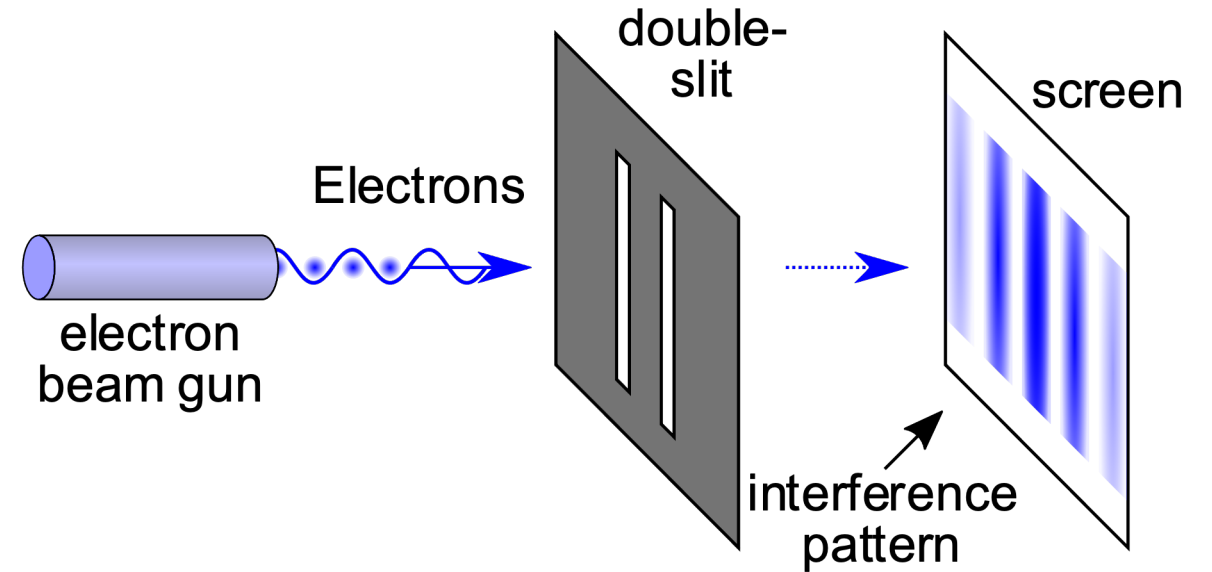
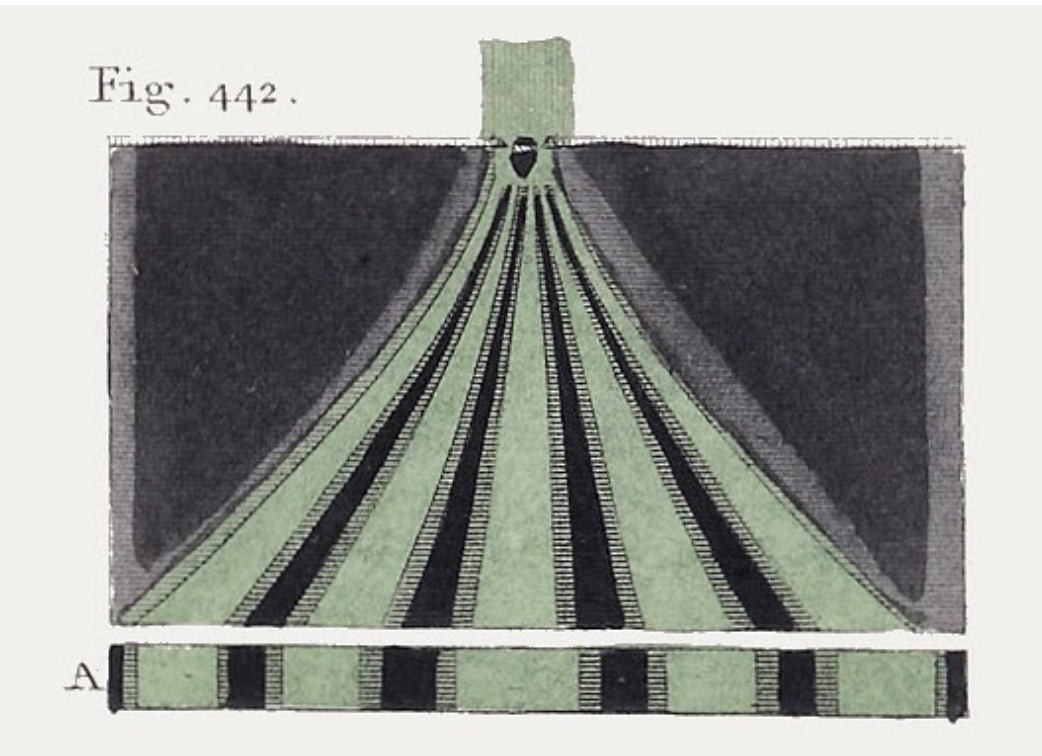
Can we get an independent estimate at RHIC?

GIULIANO GIACALONE, July 22, 2022

^{208}Pb : Jlab, RHIC?, LHC and EIC

Two weeks of RHIC Pb run

Young's double-slit experiment and the importance of phase of the wavefunction in Quantum Mechanics



The key point here is that the original source is from ONE SINGLE source.

If the electron beam gun (or laser) are two independent sources, each shots at its separate slit, there is no interference.

In QM, there is an “invisible” **phase** in particle's wavefunction in addition to the coordinates and momenta.

1799, Young's experiment demonstrates that lights are waves. (from Wikipedia)